Biochemical Journal: this is an Accepted Manuscript, not the final Version of Record. You are encouraged to use the Version of Record that, when published, will replace this version. The most up-to-date version is available at http://dx.doi.org/10.1042/BCJ20190136. Please cite using the DOI 10.1042/BCJ20190136

Comparison of type 5d autotransporter phospholipases demonstrates a correlation between high activity and intracellular pathogenic lifestyle

Running title

Comparison of type 5d-secreted phospholipases

Keywords

Autotransporter, phospholipase, phosphatidyl inositol, phosphatidyl serine, type 5d secretion system, lipids

Authors

Thomas Trunk[1], Michael A. Casasanta[2], Christopher C. Yoo[2], Daniel J. Slade[2], Jack C. Leo[1, 3*]

[1]Department of Bioscience, University of Oslo, Oslo 0316, Norway

[2]Department of Biochemistry, Virginia Polytechnic Institute and State University, Blacksburg, Virginia, VA 24061, USA

[3]Present address: Department of Biosciences, School of Science and Technology, Nottingham Trent University, Nottingham NG1 4FQ, United Kingdom

[*]corresponding author: Jack C. Leo, j.c.leo@ibv.uio.no

Abstract

Autotransporters, or type 5 secretion systems, are widespread surface proteins of Gram-negative bacteria often associated with virulence functions. Autotransporters consist of an outer membrane β-barrel domain and an exported passenger. In the poorly studied type 5d subclass, the passenger is a patatin-like lipase. The prototype of this secretion pathway is PlpD of *Pseudomonas*

Use of open access articles is permitted based on the terms of the specific Creative Commons Licence under which the article is published. Archiving of non-open access articles is permitted in accordance with the Archiving Policy of Portland Press (http://www.portlandpresspublishing.com/content/open-access-policy#Archiving).

ACCEPTED MANUSCRIPT

aeruginosa, an opportunistic human pathogen. The PlpD passenger is a homodimer with phospholipase A1 (PLA1) activity. Based on sequencing data, PlpD-like proteins are present in many bacterial species. We characterized the enzymatic activity, specific lipid binding and oligomeric status of PlpD homologs from *Aeromonas hydrophila* (a fish pathogen), *Burkholderia pseudomallei* (a human pathogen) and *Ralstonia solanacearum* (a plant pathogen) and compared these with PlpD. We demonstrate that recombinant type 5d-secreted patatin domains have lipase activity and form dimers or higher-order oligomers. However, dimerization is not necessary for lipase activity; in fact, by making monomeric variants of PlpD, we show that enzymatic activity slightly increases while protein stability decreases. The lipases from the intracellular pathogens *A. hydrophila* and *B. pseudomallei* display PLA2 activity in addition to PLA1 activity. Although the type 5d-secreted lipases from the animal pathogens bound to intracellular lipid targets, phosphatidylserine and phosphatidylinositol phosphates, hydrolysis of these lipids could only be observed for FplA of *Fusobacterium nucleatum*. Yet, we noted a correlation between high lipase activity in type 5d autotransporters and intracellular lifestyle. We hypothesize that type 5d phospholipases are intracellularly active and function in modulation of host cell signaling events.

Abbreviations

4-Mu, 4- methylumbelliferone; 4-MuH, 4-methhylumbelliferyl heptanoate; AhPlA, *Aeromonas hydrophila* phospholipase autotransporter; BAM, β-barrel assembly machinery; BpPlA, *Burkholderia pseudomallei* phospholipase autotransporter; BS3, bis(sulfosuccinimidyl)suberate; CAPS, N-cyclohexyl-3-aminopropanesulfonic acid; CvPlA, *Chromobacterium violaceum* phospholipase autotransporter; DMSO, dimethyl sulfoxide; dpi, days post-infection; DTT, dithiothreitol; EDTA, ethylenediaminetetraacetic acid; FplA, *Fusobacterium* phospholipase

autotransporter; HEPES, 4-(2-hydroxyethyl)-1-piperazineethanesulfonic acid; LB, lysogeny Broth; MES, 2-(N-morpholino)ethanesulfonic acid; MW, molecular weight; ND, not detectable; PA, phosphatidic acid; PC, phosphatidylcholine; PE, phosphatidylethanolamine; PG, phosphatidylglycerol; PI, phosphatidylinositol; PlA, phospholipase autotransporter; PLA1, phospholipase A1; PLA2, phospholipase A2; PlpD, patatin-like protein D; POTRA, polypeptide transport associated; PS, phosphatidylserine; Psi, pounds per square inch; RFU, relative fluorescence unit; RsPlA, *Ralstonia solanacearum* phospholipase autotransporter; RT, room temperature; SEC, size exclusion chromatography; T5dSS, type 5d secretion system; T5SS, type 5 secretion system; TLC, thin layer chromatography; Tris, tris(hydroxymethyl)aminomethane; VcPlA, *Vibrio cholerae* phospholipase autotransporter; wt, wild-type; ΔN, proteins lacking the N-terminal extension.

INTRODUCTION

Bacterial phospholipases comprise a diverse group of lipolytic enzymes belonging to the group of esterases. These enzymes hydrolyze glycerophospholipids and are classified based on the site of hydrolysis of their respective substrate into the subgroups phospholipase (PL)A, B, C and D. PLA is further split into PLA1 and PLA 2 depending on the site of ester bond hydrolysis at the *sn*-1 or *sn*-2 position of the glycerol moiety, respectively. PLA1 (EC 3.1.1.32) and PLA2 (EC 3.1.1.4), belonging to the group of carboxyl ester acyl hydrolases, release a fatty acid from the glycerol backbone after hydrolysis, creating second-messenger lysophospholipids, often involved in intracellular signaling pathways (1-3). Also belonging to the group of carboxyl ester acyl hydrolases, lysophospholipase A removes the remaining fatty acid thereby neutralizing the toxic effect. Phospholipases are usually secreted or membrane-associated proteins and are, in many

cases, connected to virulence in a wide range of extracellular, vacuolar and intracellular pathogens. The actual role in infection can be manifold, ranging from membrane disruption as a means for competition, colonization benefits, generating nutrients, phagosomal escape or infection establishment to the formation of bioactive molecules or membrane remodeling (4-8)

Type 5 secretion systems (T5SSs) are the most widespread secretion systems in bacteria (9) and several homologs of *plpD* have been identified by sequence similarity in various pathogenic bacteria, including *Aeromonas hydrophila*, *Burkholderia pseudomallei*, *Ralstonia solanacearum*, *Vibrio cholerae* and *Fusobacterium nucleatum*. The homolog found in *F. nucleatum*, FplA (*Fusobacterium* phospholipase autotransporter), was recently characterized as an outer membrane-associated phospholipase and thoroughly investigated in regard to enzymatic efficiency, inhibitors of lipase activity as well as lipid binding specificity (10). The *Pseudomonas aeruginosa* type 5d secretion system (T5dSS), called patatin-like protein D (PlpD), belongs to the family of patatin-like lipolytic enzymes (11). In accordance with the T5SS in general, PlpD possesses an N-terminal signal sequence for Sec-dependent translocation across the inner membrane and is dependent on the periplasmic chaperone SurA (12, 13) and presumably the BAM complex for integration of the C-terminal 16-stranded β-barrel domain into the outer membrane (9, 13-15). The β-barrel is connected by a single periplasmic polypeptide transport associated (POTRA) domain and a short linker to the N-terminal effector domain or passenger, which confers the lipolytic activity of PlpD. Once PlpD is integrated into the outer membrane, the N-terminal enzymatic domain is presumably translocated across the outer membrane through the C-terminal β-barrel domain similarly to classical autotransporters (16). Upon translocation of the passenger, the patatin-like moiety is cleaved and released into the extracellular space where it forms homodimers (17). However, not all PlpD-like patatin domains are cleaved and secreted; for

example in *Fusobacterium nucleatum*, the passenger domain can either remain attached to the β-barrel domain or is cleaved but remains associated with the bacterial surface (10).

Here we investigate, characterize and compare the passengers of T5dSSs found in several pathogenic bacteria individually and in context to already established data on phospholipase autotransporters (PlAs). We show that *plpD* homologs indeed encode for lipolytic enzymes and that oligomer formation is a conserved feature among all type 5d phospholipases tested. In spite of this, dimerization of the lipolytic domain of PlpD was found to be unnecessary for enzymatic hydrolysis of the non-native substrate 4-methylumbelliferyl heptanoate (4-MuH). Our results further show that the homolog from *Ralstonia solanacearum*, like PlpD (17), possesses **P**hospho**L**ipase **A**ctivity (PLA) 1, therefore belonging to the PLA1 carboxyl ester acyl hydrolases, whereas the homologs from *Aeromonas hydrophila* and *Burkholderia pseudomallei* possess both PLA1 and PLA2 activity, therefore being classified as phospholipase B (EC 3.1.1.5). We could also observe a correlation between temperature-dependent activity and host specificity as well as enzymatic efficiency and intracellular or extracellular pathogenic lifestyles. Although all phospholipases tested showed strong binding to phosphatidylserine (PS), the most abundant negatively charged lipid component in eukaryotic membranes (18) as well as to phosphatidic acid (PA) and to phosphatidylinositols (PI) in varying degrees, lipid hydrolysis could only be observed for FplA from *Fusobacterium nucleatum* and to a lesser degree in BpPlA from *Burkholderia pseudomallei*. Despite showing clear esterase activity towards the artificial substrate 4-MuH, determination of the specific lipid targets as well as the exact functions of PlAs *in-vivo* will need further investigation.

Materials and methods

Chemicals were ordered from Sigma-Aldrich unless otherwise specified. ExpressPlus™ 4-20% SDS-PAGE Gels were ordered from GenScript. Primers were synthesized by ThermoFisher. Sequence alterations and successful plasmid construction were confirmed by Sanger sequencing using Eurofins Genomics.

Bacterial strains and growth conditions

E. coli TOP 10 (Invitrogen) was used for amplification of target plasmids and *E. coli* BL21Gold (DE3) (Novagen) were used for protein overexpression. Bacterial strains used in this study were grown in Lysogeny Broth (LB) (19), supplemented as required with kanamycin (50 µg/mL), at 200 rpm and 37 ^{0}C. For protein overexpression, bacteria were grown for 24 h in batches of 800 mL at 30 ^{0}C with aeration in autoinducing ZYP-5052 medium (20) in the presence of 100 µg/mL kanamycin.

Production of constructs for PlA production

To produce the lipase domains of various PlAs, sequences encoding full-length PlpD (GenBank ID: AAG06727), AhPlA (AGM45846), BpPlA (ABA53592) and RsPlA (EAP74568) were codon-optimized for *E. coli* and synthesized by GeneArt (ThermoFisher Scientific). The sequences encoding the lipase domains were then subcloned into pET28a+ (Novagen) using Gibson assembly (21) to yield expression constructs containing a C-terminal histidine tag. We included the putative linker sequences in the constructs as PlpD lacking this stretch was reported

to be unstable (17). For VcPlA (AAF93770), the coding sequence was amplified directly from *V. cholerae* O1 El Tor N16961 genomic DNA and cloned into pASK-IBA3 (IBA GmbH). The lipase domain was subcloned into pET28a+ as above. To produce catalytic residue and dimerization interface point mutants, PCR-based site-directed mutagenesis was employed (22). The correctness of the constructs was determined by Sanger sequencing. Plasmids encoding the FplA lipase domain have been described before (10). All plasmids used in this study are summarized in Table 1. Primer sequences used for cloning are available upon request.

Protein expression and purification

pET28a+ plasmids containing the various expression constructs were amplified in *E. coli* TOP10 and purified using the QIAprep Spin Miniprep Kit (Qiagen) according to the manufacturer`s manual. Purified plasmids were transformed into chemically competent *E. coli* BL21Gold (DE3) and transformants were screened for on LB plates supplemented with kanamycin. For protein production, transformants were grown overnight followed by fresh inoculation of autoinducing ZYP-5052 medium (20) with starter culture at a ratio of 1:200. Cells were harvested by centrifugation at 4000 x *g* for 10 min. Pelleted cells were resuspended in buffer (40 mM Na_2HPO_4, 400 mM NaCl, pH 8.0) supplemented with EDTA-free protease inhibitor cocktail (ThermoFisher Scientific), 1 mM $MgCl_2$, 1 mM $MnCl_2$, 0.1 mg/mL lysozyme and 2 µg/mL DNase 1 before application to a French pressure cell (Thermo IEC) for three passes at 16,000 psi for cell disruption. The cell debris was pelleted by centrifugation at 20,000 x *g* for 20 min at 4 ^{0}C and the His-tagged target proteins present in the supernatant were subsequently applied to a HisTrap FF column (GE healthcare) and affinity purified using a NGC chromatography system

(BioRad) by a gradient elution with imidazole at a final concentration of 500 mM (40 mM Na_2HPO_4, 400 mM NaCl, 20-500 mM Imidazole, pH 8). Fractions containing the target proteins were confirmed to contain the correct protein by SDS-PAGE, concentrated using a centrifugal filter (Vivaspin 20, 30,000 MWCO PES) and applied to a HiPrep™ 26/60 Sephacryl® S-200 HR size exclusion column (GE) equilibrated with the protein running buffer (20 mM Tris, 300 mM NaCl, pH 7.5) for further purification. Fractions containing the target proteins were confirmed by SDS-PAGE, pooled and concentrated (Vivaspin 20, 30,000 MWCO PES). The concentration of the protein was determined based on the absorbance at 280 nm, and the solution was aliquoted in the presence of 10 % glycerol and flash-frozen in liquid nitrogen prior to storage at -80 ^{0}C.

Enzyme Kinetics

The compound 4-MuH was used as a non-native substrate for determination of enzyme activity and enzyme kinetics. 4-MuH was solubilized in 100% dimethyl sulfoxide (DMSO). Target enzymes were diluted to the respective working concentrations in reaction buffer (20 mM 2-(N-morpholino)ethanesulfonic acid (MES) pH 6/ tris(hydroxymethyl)aminomethane (Tris) pH 7.5/ 4-(2-hydroxyethyl)-1-piperazineethanesulfonic acid (HEPES) pH 8.5/ Na_2CO_3 pH 9.5/ N-cyclohexyl-3-aminopropanesulfonic acid (CAPS) pH 10.5, 50 mM NaCl, 0.5 % n-Octyl-β-D-glucoside (BOG)), added to prewarmed 96-well black microplates (Greiner Bio-one) and enzymatic activity was determined by fluorescence measurement using a Synergy H1 microplate reader (Biotek). Fluorescence (excitation at 360 nm, emission read at 449 nm) was measured after initial orbital shaking for 5 sec at a constant temperature (25^{0}C, 37^{0}C or 45^{0}C) at 2 min intervals for 20 min with 3 sec of orbital shaking before the individual reads. Cleavage of the ester bond of 4-MuH resulted in the release of 4-methylumbelliferone (4-Mu) and relative

fluorescence units measured at 449 nm were converted to product concentration using a previously established standard curve made with pure 4-Mu. Controls containing an equal amount of DMSO but no enzyme were included in all experiments and background values measured were subtracted from the data measured for the individual enzyme reactions. Enzymatic efficiency was calculated using Michaelis-Menten kinetics with the graphing and data analysis software from OriginLab (Massachusetts, USA).

Test for phospholipase activity

The EnzChek™ Phospholipase A1 Assay Kit and the EnzChek™ Phospholipase A2 Assay Kit (ThermoFisher Scientific) were used to test PLA1 and PLA2 activities according to the manufacturer's instructions. These kits provide a fluorometric method for continuous measurement of PLA1 and PLA2 activity using the specific PLA1 and PLA2 substrates PED-A1 and BODIPY® PC-A2, respectively. The final protein concentrations were adjusted for optimal signal output. Proteins from *B. pseudomallei* and *A. hydrophila* were used at a final concentration of 10 µM for detection of PLA1 activity and 50 µM for detection of PLA2 activity. Proteins from *R. solanacearum* were used at a final concentration of 50 µM and proteins from *P. aeruginosa* at a final concentration of 200 µM. The fluorescent signal measured upon substrate hydrolysis at the *sn*-1 (PLA1) and/or *sn*-2 (PLA2) position was converted to activity given in RFUs by comparison with a previously established standard curve using the PLA1/PLA2 stock solution provided by the manufacturer. Fluorescence (excitation at 470nm; emission read at 515nm) was measured using a Synergy H1 Microplate reader (BioTek).

Analytical Size Exclusion Chromatography

Analytical size exclusion chromatography (SEC) was used to estimate the molecular weight (MW) and consequently the oligomerization status of solubilized *P. aeruginosa* PlpD as well as its homologs from *A. hydrophila*, *R. solanacearum*, *B. pseudomallei* and *F. nucleatum* by creating a calibration curve using MW standards (Biorad).The range of the molecular weight markers lies between 1.35 to 670 kDa (Vitamin B12 [1.35 kDa]; Myoglobin (horse) [17 kDa]; Ovalbumin (chicken) [44 kDa]; γ-globulin (bovine) [158 kDa]; Thyroglobulin (bovine) [670 kDa]). At least 1 mg of sample was applied to a Superdex 200 Increase 10/300 GL gel filtration column (GE Life Science) using a NGC chromatography system (BioRad) in 20 mM Tris, pH 7.5, 300 mM NaCl. Samples containing BpPlA were also run in the presence of 10 mM dithiothreitol (DTT). Resulting retention times of eluted proteins were converted to MWs using the calibration curve.

Cross-linking

For in vitro cross-linking, we followed the protocol described in (23). The buffer of all purified proteins was exchanged to 10 mM HEPES, pH 7.5. To this end, protein samples were diluted in fresh 10 mM HEPES buffer and subsequently concentrated again using Vivaspin 20 concentrators (Sartorius) to a small volume. This procedure was then repeated once more. Bis(sulfosuccinimidyl)suberate (BS3) (ThermoFisher) was used as the cross-linking agent. BS3 was dissolved to 50 mM in water and 0.5 µL of this solution was added to a final volume of 30 µL 10 mM HEPES containing the target protein diluted to 1 mg/mL. The reaction was incubated at room temperature (RT) for 5 min and subsequently stopped by addition of 3 µL 1 M Tris, pH

7.5. Following a 15 min incubation at RT, 10 µL 4xSDS sample buffer was added and samples were heated to 95^{0}C for 5 min prior to application to SDS-PAGE.

Lipid binding

Membrane Lipid Strips (Echelon) were used for determination of specific lipid targeting. Following the manufacturer`s protocol, lipid strips were blocked in PBS + 2% skimmed milk powder at 4 ^{0}C overnight to avoid unspecific binding before addition of the protein of interest (PlpD S60A D207N/ AhPlA S67A D213N/ RsPlA S89A D231N: 0.5 mg/mL, BpPlA S230A D378N: 4 µg/mL) in PBS-T + 2 % skimmed milk for 1 h at RT. To avoid a loss in signal due to the lipolytic activity of the target proteins, we used double point mutant variants, where the catalytic dyad was mutated rendering the proteins catalytically inactive. Wash steps were performed with PBS-T. The primary antibody used was the mouse monoclonal THE^{TM} His Tag Antibody (GenScript) at a final concentration of 0.2 µg/mL. The secondary antibody used was CF®770 goat anti-mouse (Biotium) at a final concentration of 0.2 µg/mL. An Odyssey CLx Imaging system (LI-COR) was used for detection.

Lipid hydrolysis assay

Lipid hydrolysis assays were performed by incubation of 1 µM PlA with 0.5 mg/mL of the individual lipid in hydrolysis buffer (20 mM Na_2CO_3, 50 mM NaCl, 0.5 % BOG, pH 9.5) for 24 h at RT with aeration. After incubation, 1 volume of $CHCl_3$ was added to the samples. The sample solvent was vortexed thoroughly and shortly centrifuged. The lipid containing $CHCl_3$ phase was directly spotted on thin-layer chromatography (TLC) plates for lipid detection.

Thin layer chromatography

HPTLC silica gel 60 F_{254} plates with concentration zones (Merck) were used for TLC to separate digested lipids. TLC plates were incubated at 100 °C for one hour for activation by removal of any absorbed moisture before usage. Plates were allowed to cool down before samples were applied as small dots on the upper half of the concentration zone using glass micropipettes (Brand®). A sample volume of 10 µL was spotted and the sample solvent was allowed to evaporate completely before transferring the plate to the TLC chamber. A solvent system containing H_2O, methanol and $CHCl_3$ with a volume mixing ratio of 4:27:65 was used as mobile phase in the case of PE and PS, whereas the ratio was adjusted to 4:28:65 in the case of PI(4)P and the soy lipid extract. The atmosphere within the TLC chamber was saturated for at least one hour prior to plate application. The plate was removed from the TLC chamber before the mobile phase could reach the top of the plate and air dried until complete evaporation of the solvent. Exposing the TLC plate to iodine vapor was used as to visualize separated lipids. Iodine crystals were placed into the iodine chamber 24 h before use to assure complete saturation of the chamber with iodine vapor. After staining, the plates were digitized by scanning.

Toxicity assays using *Galleria mellonella*

Galleria mellonella TruLarv® larvae were obtained from BioSystems Technology. The direct toxic effect of PlAs was tested by intrahemocoelic injection (24) of 20 µL purified protein of varying concentrations in PBS using a single syringe infusion pump (Cole-Parmer). The control groups were injected with either the respective, catalytically dead enzyme or 20 µL PBS. Larvae, each weighing 0.2-0.3 g, were kept at 37^0C for 5 days and were checked for stages of disease/survival in a 24 h interval. Dead larvae, detectable by strong melanization and lack of movement, were removed from the stock of surviving larvae. Percentage survival was plotted

against concentration for each of the concentration of PlA tested, and lethal dose (LD50) values were calculated using origin (25).

Bioinformatics

Bioinformatic analyses were mostly performed using online tools at the Max Planck Institute Bioinformatics Toolbox (26). Sequence searches were performed using BLAST or PSI-BLAST (27) using the PlpD or BpPlA sequences as queries. Sequence alignments were performed with Clustal Ω (28) followed by manual editing. Secondary structure prediction was done using Ali2D (26). For predicting signal sequences, SignalP 4.1 (29) and Phobius (30) were employed. In some cases (e.g. AGM45846), the start codon was apparently mis-annotated; therefore, manual scanning of the upstream sequence was instigated until a well-predicted in-frame signal peptide was located.

Mass Spectrometry

In-gel trypsin digest of gel-fractionated target proteins were analyzed by mass spectrometry using the proteomic facilities at the University of Oslo (https://www.mn.uio.no/ibv/english/research/sections/bmb/research-groups/enzymology-and-protein-structure-and-function/proteomics-thiede/proteomics-service/)

RESULTS

Sequence analysis of passengers of PlpD homologs

Many species of bacteria contain genes homologous to *plpD*, including members of the Proteobacteria, Bacteroidetes, Firmicutes and Chlorobi (11). The passengers of the proteins encoded by these genes represent a patatin-like lipase domain and are all highly similar to PlpD. An alignment of selected lipase domains demonstrates this similarity, especially at the level of predicted secondary structure (Figure 1). The alignment pinpoints the conserved catalytic dyad (serine, aspartic acid) as well as the few residues forming the oxyanion hole, suggesting that they all possess lipase activity, similar to PlpD and FplA (10, 17). Following the convention established for FplA, we have named this group of proteins Phospholipase Autotransporters (PlAs), and included the first two letters of the binomial names to designate the source species. Thus, the PlA from *Aeromonas hydrophila* is named AhPlA, the PlA from *Vibrio cholerae* VcPlA, and so forth. To avoid confusion in the literature, we have kept the name PlpD for the *P. aeruginosa* protein, and FplA for the *Fusobacterium nucleatum* PlA.

All PlAs have a predicted signal peptide at the N-terminus. For most, this is between 18 and 23 residues in length, a standard length for Sec-dependent signal peptides. However, CvPlA (from *Chromobacterium violaceum*), RsPlA (from *Ralstonia solanacearum*) and the PlA from *Burkholderia pseudomallei* (BpPlA) have longer signal sequences, 29, 30 and 36 residues, respectively (Figure 1B). Some autotransporters of other classes also have extended signal sequences (31, 32), and the signal peptides of BpPlA and CvPlA are reminiscent of those.

Most of the proteins shown in Figure 1B contain just the lipase domain preceding the putative linker sequence connecting to the periplasmic POTRA domain. However, some PlAs have an N-terminal extension. FplA has a 40-residue extension (10), but BpPlA has a significantly longer extension (155 residues). This region contains a number of alanine and serine-rich repeats (Figure 1B). Such extensions are found in all *B. pseudomallei* PlAs, though the number of these repeats

varies between strains (Figure S1). Similar extensions are also present in the closely related *B. mallei*, but other members of the *Burkholderia* genus have PlAs with significantly shorter extensions (Figure S1).

Predicted *plpD* homologs encode for a type 5d phospholipase autotransporters

The sequences coding for the passenger of AhPlA, BpPlA, PlpD, RsPlA and VcPlA lacking the N-terminal signal sequence were cloned into the expression plasmid pET28+, which provides a C-terminal His-tag, and expressed in *E. coli* BL21Gold(DE3). The proteins were then purified by affinity and size exclusion chromatography. In contrast to the other PlAs, VcPlA was only produced as inclusion bodies. As our attempts at refolding VcPlA failed (data not shown), we did not analyse this protein further. For the other PlAs, esterase activity was determined by continuous fluorometric measurement using the non-native lipid substrate 4-MuH (Figure 2A).

All purified proteins were active and esterase activity could be shown for PlpD as well as all homologs with a functional catalytic dyad (Table 2; Figure 2A). Although the Michaelis constant (K_m) was at a comparable level for most of the tested PlAs, the substrate turnover rates (k_{cat}) varied significantly ranging from a comparatively low value of k_{cat} ~0.1 s^{-1} and ~0.3 s^{-1} in the case of the RsPlA passenger and the PlpD passenger, respectively, to a k_{cat} ~21 s^{-1} for the BpPlA passenger. During purification, we noticed some apparent degradation of the PlAs, particularly in the case of RsPlA (Figure S2). We also observed minor degradation products in the case of BpPlA (Figure S2). We were concerned that this might affect the enzyme activity; therefore, we mapped the degradation site to the N-terminus of RsPlA by mass spectrometry (Figure S2). We then produced a protein, corresponding to the degradation product, lacking the N-terminal

extension (RsPlA ΔN). Deletion of the N-terminal extensions of the BpPlA and RsPlA passengers, resulting in the proteins BpPlA ΔN and RsPlA ΔN, led only to a slight decrease in enzymatic efficiency by roughly a factor of two (Table 2), therefore, we assumed that the degradation of RsPlA has no major effect on the protein`s enzymatic activity. Upon the dual mutation of the active site Serine (Ser→Ala) and Aspartate (Asp→Asn) of the catalytic dyad, enzymatic activity decreased significantly or was completely abolished in all PlAs (Table 2).

PlAs display enzymatic activity across a broad pH and temperature range

Enzyme kinetics at a range of biologically relevant temperatures and pH values were performed to determine the optimum conditions for activity of the purified passengers of PlpD, AhPlA, BpPlA/BpPlA ΔN and RsPlA/RsPlA ΔN (Figure 2A, Figure S3).

Enzymatic activity could be detected along a broad pH range (pH 6 – pH 10) for all PlAs with a pH optimum for the different proteins between pH 8.5 and pH 9.5. A clear drop in activity could be observed at pH values above 9.5 or below 8 (Figure S3). In the case of BpPlA, the N-terminal extension was important in oligomer formation (see below). No significant difference in pH-dependent activity could be observed between BpPlA and BpPlA ΔN. RsPlA ΔN was included in the experiment after the observation of a degradation product of RsPlA during SDS-gel fractionation (Figure S2). RsPlA ΔN showed a decrease in enzymatic efficiency compared to the RsPlA wild-type (wt) protein at all points, ranging from a factor of two at pH 6 to a factor of 10 at pH 10.

PlpD, BpPlA and BpPlA ΔN are also active at a broad temperature spectrum ranging from 25-45 ^{0}C with an optimum in enzymatic efficiency of 1.8 x 10^{3} s^{-1} M^{-1}, 6.9 x 10^{5} s^{-1} M^{-1} and 2.6 x 10^{5}

s^{-1} M^{-1} at 37^0C, respectively (Table 2). A decrease in enzymatic efficiency is correlated with an increase in temperature in the case of AhPlA and RsPlA, with the highest enzymatic activity of 8.8 x 10^4 s^{-1} M^{-1} (AhPlA) and 7.9 x 10^3 s^{-1} M^{-1} (RsPlA) at 25 ^{0}C (Table 2). BpPlA ΔN showed only a minor decrease in enzymatic activity by roughly a factor of two when compared to BpPlA wt. RsPlA ΔN on the other hand showed no detectable activity at 45 ^{0}C (Figure S3).

PlAs from *A. hydrophila* and *B. pseudomallei* have phospholipase B activity

Phospholipase activities are subdivided into phospholipase A, B, C and D according to the specific site of hydrolysis on a phospholipid. In this context, all PlAs were tested for PLA1 and PLA2 activity using PLA1 and PLA2-specific substrates.

All PlAs showed activity towards the PLA1-specific substrate PED-A1 (Figure 2B). A strong activity was measured for BpPlA (>4 Relative Fluorescence Units (RFUs)), RsPlA (>4 RFUs) and AhPlA (>3 RFUs) at a molecular concentration of 20 µM, 50 µM and 20 µM, respectively. PlpD on the other hand showed a comparable activity of >6 RFUs only after 1h and at a final concentration of 200 µM. The lower activity observed for PlpD is in agreement with previous results, where the PLA1 activity of PlpD, although clear, was significantly lower than the positive control (17). PLA1 activity increased with time for all PlAs, whereas the catalytically impaired variants of the same proteins (AhPlA S67A D213N, BpPlA S230A D378N, PlpD S60A D207N and RsPlA S89A D231N) displayed no PLA1 activity (Figure 2B).

The PlAs from *A. hydrophila* and *B. pseudomallei* also displayed PLA2 activity (Figure 2B). A high activity (AhPlA ~7 RFUs; BpPlA >4 RFUs) was evident in both cases, whereas no activity could be detected for RsPlA or PlpD.

Binding to phosphatidylserine is conserved in PlAs

After confirmation of lipolytic activity for as well as enzymatic characterization of all PlAs using the non-native lipid substrate 4-MuH, we wanted to identify the native interaction partners of the individual proteins. To this end, lipid binding assays were performed individually for all PlAs using lipid-coated strips covering the most abundant phospholipids present in eukaryotic and prokaryotic cells (Figure 3). We used the catalytically inactive versions of the respective PlAs to avoid loss of signal due to hydrolysis of the target lipids bound to the lipid strips. We also tested the binding of wt PlpD to the lipid strip and did not observe any significant differences to the mutant, thus confirming that mutation of the catalytic dyad has no major effect on lipid binding (Figure S4).

AhPlA S67A D213N, BpPlA S230A D378N and RsPlA S89A D231N all bound PS with relatively high affinity compared to the other phospholipids tested, as well as to PA, although less strongly (Figure 3). Our results for PlpD were qualitatively similar to those observed previously (17). None of the PlAs tested showed binding towards phosphatidylethanolamine (PE), phosphatidylcholine (PC), phosphatidylglycerol (PG), or phosphatidylinositol (PI) without additional phosphorylation of the inositol group. PI 4-phosphate (PI(4)P), PI (4,5)-biphosphate (PI(4,5)P_2) and PI (3,4,5)-triphosphate (PI(3,4,5)P_3) binding was observed for PlpD S60A D207N and AhPlA S67A D213N. BpPlA S230A D378N only bound to PI(4)P, whereas no binding was detected between any phosphoinositol and RsPlA S89A D231N. AhPlA S67A D213N was the only one of the tested proteins to bind to cardiolipin in our experiments. We did not see any binding of PlpD to cardiolipin, in contrast to what was observed both for PlpD (17) and FplA

(10). Although FplA did bind to cardiolipin, it did so only at high lipid concentrations of (10). We suggest that PlA binding to cardiolipin might be an artifact, e.g. due to dose-dependent unspecific binding.

Thin layer chromatography

To ascertain that the lipids that bound to PlAs are also targets for hydrolysis, we perfomred enzymatic digestions of purified lipids. We chose PS and PI(4)P, as these were targeted by most PlAs in the lipid overlay assays. We also included PE as a non-target lipid. Surprisingly, only FplA showed clear hydrolytic activity towards both PE and PS, where one of two bands disappeared during incubation with the active enzyme. No activity was detected towards PI(4)P for any of the lipases (Figure 4A-C).

As we did not observe any hydrolysis with specific lipids, we then tested a mix of lipids. For this, we used a soy bean polar lipid mix (PC 45.7 %; PE 22.1 %; PI 18.4 %; PA 6.9 %; unknown lipids 6.9 %; Avanti).

The soy lipid extract showed three distinctive bands in the absence of any PlA. When incubated with FplA, the upper and the lower band disappeared or at least a strong reduction in intensity was observed (Figure 4D). Similarly to FplA, also BpPlA showed hydrolytic activity towards the upper band present in the soy lipid extract. Although far less pronounced compared to FplA, a reduction in intensity of the upper band could be observed (Figure 4D) which is absent in BpPlA S230A D378N. The other PlAs showed no detectable activity towards any of the major lipid species tested at the given concentration (Figure 4D).

Formation of homodimers is conserved within PlAs

The PlpD passenger structure has an α/β hydrolase fold with a twisted six-stranded central β-sheet surrounded by eight major helices, which forms homodimers due to the direct interaction between the two hydrophobic α7-helices of neighbouring molecules (17) (Figure 5A). Sequence alignments of *plpD* and its homologs revealed that the interaction interface is conserved within the tested PlAs (Figure 5A). To investigate the potential oligomerization of the purified passengers, we employed SEC in combination with cross-linking experiments using BS3. The estimated molecular sizes of the monomeric target proteins were determined using Protparam (ExPASy) and are shown in Table 3.

The MW estimated by SEC for the purified passengers of PlpD, AhPlA, RsPlA and $FplA_{20-431}$ (10) in solution were 69 kDa, 62 kDa, 65 kDa and 83 kDa, respectively (Figure 5C). The estimated MWs correspond to approximately twice that of the MWs of the monomeric proteins (Figure 5D). Mutation of the catalytic dyad residues, resulting in the catalytically impaired AhPlA S67A D213N and RsPlA S89A D231N, had no significant effect on the MW compared to the respective wt constructs (Table 3), demonstrating that the introduced mutations do not have an effect on dimerization and folding of mutant proteins.

In the case of BpPlA, we observed a very large protein aggregate under oxidizing conditions. Because BpPlA contains a single cysteine in the N-terminal extension, we reasoned that the aggregation may be due to disulphide cross-linking. To test this, we repeated the experiment in the presence of the reducing agent DTT. Under these conditions, the MW of the BpPlA passenger was estimated to be approximately four times the size of the monomeric BpPlA, at 191 kDa (Figure 5C & D). The MW of the catalytically impaired BpPlA S230A D378N was determined to

be in a similar range with an estimated MW of 178 kDa. Deletion of the N-terminal extension, resulting in the truncated protein BpPlA ΔN, resulted in loss of aggregation and a significant decrease in molecular size with an estimated MW of 60 kDa in solution, corresponding to a dimeric protein. Thus, the N-terminal extension promotes potential dimer-dimer formation but is not needed for homodimer formation.

The amine-amine crosslinker BS3 was used to confirm multimer formation of the purified PlAs. Successful cross-linking of all PlAs was detected after addition of BS3, whereas no SDS-resistant multimer formation was observed in absence of the cross-linking agent (Figure 5B). A clear cross-linking product at a MW of approximately 100 kDa could be detected for the PlpD, RsPlA, AhPlA and FplA passengers. The additional band at 25 kDa in the case of RsPlA shows the previously mentioned RsPlA degradation product. The BpPlA passenger sample showed a prominent band roughly at 200 kDa as well as minor bands at approximately 150 kDa and 120 kDa. In the case of BpPlA pass ΔN one distinctive cross-linking product at approximately 100 kDa could be detected, which corresponds to the bands of dimeric PlpD, RsPlA and AhPlA. The identity of the bands indicating formation of multimers were confirmed by MS (Figure S5)

PlpD can be stably monomerised by disrupting the hydrophobic dimerization interface

To investigate the role of homodimer formation in enzyme activity, specific residues at the reported interaction interface on helix α7 (Figure 6A) were substituted, resulting in the mutants PlpD M249E and PlpD I253A M256D. Both mutants resulted in stable monomeric protein as shown by SEC (Figure 6B) and BS3 cross-linking (Figure 6C). The wt PlpD showed a prominent band at approximately 100 kDa following incubation with BS3 during the cross-linking

experiment which is absent in the monomeric PlpD I253A M256D. In PlpD M249D a faint band is still visible at aprroximately 100 kDa. Independent of BS3, both monomeric proteins showed an additional band at 25 kDa which is absent in the PlpD dimer. These are of a similar size as the degradation product of RsPlA, which led us to assume that the additional band is a degradation product of the PlpD monomers. SEC provided corroborating results for the mutants being monomers, where PlpD M249E as well as PlpD I253A M256D eluted at an estimated size of 35 kDa, the expected size of the monomer (Table 4). By contrast, the PlpD passenger eluted at an estimated MW of 69 kDa, corresponding to a dimeric protein.

Homodimer formation by PlpD is not necessary for lipase activity in vitro

The monomeric PlpD variants were tested for alteration or loss in enzymatic activity using 4-MuH. Both PlpD M249E and PlpD I253A M256D showed slightly increased lipase activity at lower temperatures compared to the homodimer, demonstrating that the monomeric variants are enzymatically active (Table 5). Although showing comparable enzymatic efficiencies at lower temperatures, PlpD monomers showed a marked decrease in enzymatic activity with increasing temperatures, which was not observed with the PlpD dimer, as it was stably active up to 45 ^{0}C (Figure 7). The same trend was observed when testing for PLA1 activity. When comparing PLA1 activity of the proteins, a slight but clear increase in activity of the monomeric proteins PlpD M249E (<3 RFU) and PlpD I253A M256D (<3 RFU) compared to dimeric PlpD (<1 RFU) was detected at all time points (Figure 7).

Low toxic effect of AhPlA and BpPlA on survival of *Galleria mellonella*

The insect *G. mellonella* belongs to the order *Lepidoptera* and the family *Pyralidae* (Scoble M. Classification of the Lepidoptera Oxford University Press, 1995). The use of the caterpillar larvae of G. mellonella as an animal model for microbial infections attracts increasing attention due to remarkable similarities of their innate immune response with the immune response in vertebrates (33) while being inexpensive and easy to handle (34).

The direct toxic effect of PlAs was tested by intrahemocoelic injection of purified protein into *Galleria mellonella* larvae. The mortality rate of larvae as response to injection with BpPlA and AhPlA were dose dependent. Whereas no toxic effect of either of the two PlAs was observed 5 days post-infection (dpi) with 2 µg/g, an increase of dosage to 20 µg/g resulted in a mortality rate of 25 % in the case of BpPlA and 19 % in the case of AhPlA. By increasing the dosage to 200 µg/g, mortality rates also increased to 40 % for BpPlA and 22 % for AhPlA.

Neither PlpD (1 mg/g) nor FplA (125 µg/g) showed any toxic effect, even at very high concentrations (Table S1).

DISCUSSION

The type 5d subclass of autotransporters was described almost 10 years ago, with PlpD from *Pseudomonas aeruginosa* as the prototype (11). PlpD consists of a C-terminal outer membrane-embedded 16-stranded β-barrel connected to a single POTRA domain, a short linker and an N-terminal passenger. The passenger belongs to the family of bacterial patatin-like phospholipases, forming homodimers upon translocation across the outer membrane and release into the extracellular space (17). T5SSs as well as bacterial phospholipases are important pathogenicity

factors employed by many organisms during infection. Despite this potential biological relevance, little is known about PlpD and little to no information is available on PlpD homologs in other organisms. FplA from *Fusobacterium nucleatum* is the lone exception, which was recently characterized (10) .

Based on sequence alignments, homologs of PlpD found in *A. hydrophila*, *B. pseudomallei* and *R. solanacearum* were tested and confirmed for esterase activity due to the recognition and subsequent hydrolysis of the artificial substrate 4-MuH. Like PlpD (11) and FplA (10), all tested passengers share a conserved serine-aspartate catalytic dyad necessary for enzymatic activity, as demonstrated by loss of activity when these residues are mutated. Although highly similar in structure and primary sequence, RsPlA, BpPlA and FplA have distinctive differences when compared to PlpD, e.g. the N-terminal extension of their respective passengers. Deletion of the N-terminal extension had almost no effect on the enzymatic activity. We therefore speculate that the N-terminal extensions could have a role in folding or structural stabilization or possibly in binding to target molecules or membranes. This is supported by the fact that the deletion of the N-terminal extension in *R. solanacearum* led to a decrease in thermal stability at increasing temperatures, as well as the fact that PlAs from *B. pseudomallei* with intact N-termini form higher molecular-weight complexes, as demonstrated by SEC and cross-linking experiments. This observation indicates a role for the extension in multimer formation. The particularly long N-terminal extensions found in the proteins from the highly virulent *B. pseudomallei* and *B. mallei*, combined with the conspicuous lack in orthologs from less pathogenic *Burkholderia* species, also points to a role in virulence. Multimer formation by self-association of proteins can confer structural or functional advantages, e.g. increased stability, heightened substrate specificity or regulation of enzymatic activity. Although homodimer formation is a conserved

feature of the tested PlAs, it is not needed for enzyme activity of PlpD. Both mutants, PlpD M249E and PlpD I253A M256D, were enzymatically active in their monomeric form. When exposed to an increase in temperature, however, the monomers show a drastic decrease in enzymatic efficiency, while the activity of the dimer stays at a comparable level over a broad temperature range. Dimerization of PlpD therefore increases stability and assures enzymatic activity over a broad temperature range, but we cannot exclude that the lower activity of the dimer also plays another role. Homodimer formation may result in conformational changes, which enables the highly specific binding of individual lipid targets or the generation of sites for allosteric regulation, allowing the binding of cofactors to non-substrate sites (35, 36).

Upon translocation across the outer membrane, passengers can either stay attached to the membrane or be cleaved off and released into the extracellular space, as has been reported for PlpD (11). FplA from *F. nucleatum* is cleaved in some strains, but not released from the membrane (10). Although not impossible, the fact that all tested PlA passengers form homodimers or, in the case of BpPlA, complexes of more than 2 subunits, makes it unlikely that PlAs in general stay surface-attached and suggests protein cleavage upon translocation across the outer membrane. Especially the probable dimer-dimer formation by BpPlA seems unlikely to take place while still attached to the membrane. If the lipase domains are indeed released by proteolysis, this is most likely facilitated by an external protease, based on the observation that neither the PlpD nor the FplA passenger is cleaved after heterologous expression in *E. coli* (10, 11).

Interestingly, the activities of the various type 5d lipases towards 4-MuH are correlated with the lifestyle of the source bacteria: PlAs from mainly extracellular pathogens such as *P. aeruginosa* had comparatively low activity, whereas the intracellular pathogens *F. nucleatum* (10) and *B.*

pseudomallei displayed much higher activity. PlAs from the extracellular pathogens *P. aeruginosa* and *R. solanacearum* (37-39) showed a low enzymatic efficiency when exposed to 4-MuH compared to those from the intracellular pathogens *B. pseudomallei* (40), *F. nucleatum* (10) and the facultative intracellular pathogen *A. hydrophila* (41, 42). This activity difference may indicate a primarily intracellular role for the type 5d phospholipases. Although further research into this topic is necessary, possible roles may include interference with signal transduction pathways, similar to the case of the *P. aeruginosa* ExoU (43, 44), or phagosomal escape into the cell cytosol similar to other phospholipases (7, 8, 45). However, given the low activity of PlAs towards major lipids, the latter does not seem to be a very likely function of PlAs.

In spite of strong PS binding by all tested proteins, hydrolysis of the purified lipids could only be observed in the case of FplA incubated with PE or PS. PS is the most abundant negatively charged phospholipid in eukaryotic cells and is largely spatially restricted to the cytosolic side of the cell membrane (18). In bacterial membranes, PS is less abundant or absent, but nonetheless an important cytosolic precursor in the synthesis of essential membrane lipids like PE in *E. coli* through the two enzymes phosphatidylserine synthase and phosphatidylserine decarboxylase (46). Next to its role in PE synthesis, PS is also a known target lipid for a range of specific membrane binding proteins (47). Thus, PS might not be a target for digestion by PlAs, but might be a binding target that guides PlAs to membranes where they then act on their specific target(s). In our digestion assays, only the highly active lipases FplA and BpPlA had any detectable activity. The in vivo targets of PlAs thus still remain to be discovered.

It should be noted that FplA only removed one of several PS or PE bands, suggesting that the acyl chain identity could also affect target specificity. The hydrophobic cleft of PlpD can

accommodate C_{18}-C_{20} acyl chains (17).Thus, the size of the chain and the presence and position of unsaturated bonds could affect lipid specificity.

None of the tested PlAs showed hydrolytic activity towards PI(4)P at the given concentrations, despite previous studies suggesting phosphorylated PIs might be the targets of PlAs (10, 17). PIs are most abundant in the cytosolic membrane leaflets and play essential roles in eukaryotes. These roles include their function as membrane-located interaction partners for a wide range of proteins involved in cellular signal transduction cascades (48, 49). Though we did not observe hydrolysis of PI(4)P in our experiments, we did not test other PI species. Therefore, we cannot exclude other phosphorylated PI species as possible interaction partners in vivo..

The lack of PlA-mediated PE or PS digestion, with the exception of FplA, makes it unlikely that the tested PlAs target major lipid species. Nonetheless, the tested PlAs may target minor lipid species or may need yet unidentified cofactors for full activity not present in the commercially available lipid extracts. This idea is supported by the fact that hydrolysis of certain lipids present in the soy extract was observed after incubation with FplA and BpPlA. Especially BpPlA, which did not show hydrolytic activity towards purified PE, PS or PI(4)P, showed lipolytic activity when confronted with a mixture of lipids present in the soy extract.

When it comes to the specific cleavage site engaged by the tested phospholipases, RsPlA cleaves at the *sn*-1 position, therefore belonging to the group of 1-acyl hydrolyses, as previously shown for PlpD (17) The passengers of BpPlA and AhPlA possess both PLA1 and PLA2 activity, therefore belonging to the group of phospholipases B. Interestingly, only the PlAs with PLB activity demonstrated any toxicity in the *Galleria* model. Even then, toxicity required very high protein concentrations, demonstrating that PlAs are most likely not membrane-disrupting toxins.

This is fully in line with our in vitro observations and suggests that PlAs play much more subtle roles in vivo. Taken together, the higher activity of PlAs from intracellular pathogens, the apparently narrow substrate range, and the low toxicity of PlAs point towards a very specific, possibly intracellular role for these proteins in virulence. We therefore propose a role in modulating host signaling events during intracellular infections as a hypothesis for future research.

Acknowledgements

We would like to thank Professor Dirk Linke as well as the members of his group at the University of Oslo for discussions and support and Jan Haug Anonsen at the Proteomics Facility at the University of Oslo for his help with mass spectrometry. We thank Associate Professor Melanie Blokesch (EPFL – École polytechnique fédérale de Lausanne, Switzerland) for providing the *V. cholerae* DNA. This study was funded by the Norwegian Research Council Young Investigator grant 249793 (to JCL), and the USDA National Institute of Food and Agriculture (DJS).

Ethics Statement

The work involving *Galleria mellonella* does not need ethical permission according to Norwegian law. The authors state no conflict of interest.

Author Contributions

JCL conceived and JCL, DJS and TT designed the study. TT, MAC, CCY performed the enzymology experiments. JCL did the molecular cloning and mutagenesis. TT performed all other experiments. TT and JCL wrote the initial draft and all authors contributed to the final written manuscript.

References

1. Richmond GS, Smith TK. Phospholipases A(1). Int J Mol Sci. 2011;12(1):588-612.
2. Newton AC, Bootman MD, Scott JD. Second Messengers. Cold Spring Harb Perspect Biol. 2016;8(8).
3. Paul RU, Holk A, Scherer GFE. Fatty acids and lysophospholipids as potential second messengers in auxin action. Rapid activation of phospholipase a(2) activity by auxin in suspension-cultured parsley and soybean cells. Plant J. 1998;16(5):601-11.
4. Istivan TS, Coloe PJ. Phospholipase A in Gram-negative bacteria and its role in pathogenesis. Microbiology. 2006;152(Pt 5):1263-74.
5. Berstad AE, Berstad K, Berstad A. PH-activated phospholipase A2: an important mucosal barrier breaker in peptic ulcer disease. Scand J Gastroenterol. 2002;37(6):738-42.
6. Schmiel DH, Wagar E, Karamanou L, Weeks D, Miller VL. Phospholipase A of Yersinia enterocolitica contributes to pathogenesis in a mouse model. Infect Immun. 1998;66(8):3941-51.
7. Jamwal SV, Mehrotra P, Singh A, Siddiqui Z, Basu A, Rao KV. Mycobacterial escape from macrophage phagosomes to the cytoplasm represents an alternate adaptation mechanism. Sci Rep. 2016;6:23089.
8. Tonello F, Zornetta I. Bacillus anthracis factors for phagosomal escape. Toxins (Basel). 2012;4(7):536-53.
9. Leo JC, Grin I, Linke D. Type V secretion: mechanism(s) of autotransport through the bacterial outer membrane. Philos Trans R Soc Lond B Biol Sci. 2012;367(1592):1088-101.
10. Casasanta MA, Yoo CC, Smith HB, Duncan AJ, Cochrane K, Varano AC, et al. A chemical and biological toolbox for Type Vd secretion: Characterization of the phospholipase A1 autotransporter FplA from Fusobacterium nucleatum. J Biol Chem. 2017;292(49):20240-54.
11. Salacha R, Kovacic F, Brochier-Armanet C, Wilhelm S, Tommassen J, Filloux A, et al. The Pseudomonas aeruginosa patatin-like protein PlpD is the archetype of a novel Type V secretion system. Environ Microbiol. 2010;12(6):1498-512.
12. Klein K, Sonnabend MS, Leibiger K, Franz-Wachtel M, Macek B, Trunk T, et al. Deprivation of the Periplasmic Chaperone SurA Reduces Virulence and Restores Antibiotic Susceptibility of Multidrug-Resistant Pseudomonas aeruginosa.". Front Microbiol. 2019.

659 13. Sauri A, Soprova Z, Wickstrom D, de Gier JW, Van der Schors RC, Smit AB, et al. The Bam (Omp85)
660 complex is involved in secretion of the autotransporter haemoglobin protease. Microbiology.
661 2009;155(Pt 12):3982-91.
662 14. Ieva R, Bernstein HD. Interaction of an autotransporter passenger domain with BamA during its
663 translocation across the bacterial outer membrane. Proc Natl Acad Sci U S A. 2009;106(45):19120-5.
664 15. Ieva R, Tian P, Peterson JH, Bernstein HD. Sequential and spatially restricted interactions of
665 assembly factors with an autotransporter beta domain. Proc Natl Acad Sci U S A. 2011;108(31):E383-91.
666 16. Fan E, Chauhan N, Udatha DB, Leo JC, Linke D. Type V Secretion Systems in Bacteria. Microbiol
667 Spectr. 2016;4(1).
668 17. da Mata Madeira PV, Zouhir S, Basso P, Neves D, Laubier A, Salacha R, et al. Structural Basis of
669 Lipid Targeting and Destruction by the Type V Secretion System of Pseudomonas aeruginosa. J Mol Biol.
670 2016;428(9 Pt A):1790-803.
671 18. Leventis PA, Grinstein S. The distribution and function of phosphatidylserine in cellular
672 membranes. Annu Rev Biophys. 2010;39:407-27.
673 19. Bertani G. Studies on lysogenesis. I. The mode of phage liberation by lysogenic Escherichia coli. J
674 Bacteriol. 1951;62(3):293-300.
675 20. Studier FW. Protein production by auto-induction in high density shaking cultures. Protein Expr
676 Purif. 2005;41(1):207-34.
677 21. Gibson DG, Young L, Chuang RY, Venter JC, Hutchison CA, 3rd, Smith HO. Enzymatic assembly of
678 DNA molecules up to several hundred kilobases. Nat Methods. 2009;6(5):343-5.
679 22. Liu H, Naismith JH. An efficient one-step site-directed deletion, insertion, single and multiple-site
680 plasmid mutagenesis protocol. BMC Biotechnol. 2008;8:91.
681 23. Leo JC, Oberhettinger P, Chaubey M, Schutz M, Kuhner D, Bertsche U, et al. The Intimin
682 periplasmic domain mediates dimerisation and binding to peptidoglycan. Mol Microbiol. 2015;95(1):80-
683 100.
684 24. Ramarao N, Nielsen-Leroux C, Lereclus D. The insect Galleria mellonella as a powerful infection
685 model to investigate bacterial pathogenesis. J Vis Exp. 2012(70):e4392.
686 25. Megaw J, Thompson TP, Lafferty RA, Gilmore BF. Galleria mellonella as a novel in vivo model for
687 assessment of the toxicity of 1-alkyl-3-methylimidazolium chloride ionic liquids. Chemosphere.
688 2015;139:197-201.
689 26. Zimmermann L, Stephens A, Nam SZ, Rau D, Kubler J, Lozajic M, et al. A Completely
690 Reimplemented MPI Bioinformatics Toolkit with a New HHpred Server at its Core. J Mol Biol.
691 2018;430(15):2237-43.
692 27. Altschul SF, Koonin EV. Iterated profile searches with PSI-BLAST--a tool for discovery in protein
693 databases. Trends Biochem Sci. 1998;23(11):444-7.
694 28. Sievers F, Higgins DG. Clustal Omega for making accurate alignments of many protein sequences.
695 Protein Sci. 2018;27(1):135-45.
696 29. Petersen TN, Brunak S, von Heijne G, Nielsen H. SignalP 4.0: discriminating signal peptides from
697 transmembrane regions. Nat Methods. 2011;8(10):785-6.
698 30. Kall L, Krogh A, Sonnhammer EL. A combined transmembrane topology and signal peptide
699 prediction method. J Mol Biol. 2004;338(5):1027-36.
700 31. Szabady RL, Peterson JH, Skillman KM, Bernstein HD. An unusual signal peptide facilitates late
701 steps in the biogenesis of a bacterial autotransporter. Proc Natl Acad Sci U S A. 2005;102(1):221-6.
702 32. Desvaux M, Scott-Tucker A, Turner SM, Cooper LM, Huber D, Nataro JP, et al. A conserved
703 extended signal peptide region directs posttranslational protein translocation via a novel mechanism.
704 Microbiology. 2007;153(Pt 1):59-70.
705 33. Browne N, Heelan M, Kavanagh K. An analysis of the structural and functional similarities of
706 insect hemocytes and mammalian phagocytes. Virulence. 2013;4(7):597-603.

34. Tsai CJ, Loh JM, Proft T. Galleria mellonella infection models for the study of bacterial diseases and for antimicrobial drug testing. Virulence. 2016;7(3):214-29.
35. Marianayagam NJ, Sunde M, Matthews JM. The power of two: protein dimerization in biology. Trends Biochem Sci. 2004;29(11):618-25.
36. Mei G, Di Venere A, Rosato N, Finazzi-Agro A. The importance of being dimeric. FEBS J. 2005;272(1):16-27.
37. Digonnet C, Martinez Y, Denance N, Chasseray M, Dabos P, Ranocha P, et al. Deciphering the route of Ralstonia solanacearum colonization in Arabidopsis thaliana roots during a compatible interaction: focus at the plant cell wall. Planta. 2012;236(5):1419-31.
38. Ferreira V, Pianzzola MJ, Vilaro FL, Galvan GA, Tondo ML, Rodriguez MV, et al. Interspecific Potato Breeding Lines Display Differential Colonization Patterns and Induced Defense Responses after Ralstonia solanacearum Infection. Front Plant Sci. 2017;8:1424.
39. Moradali MF, Ghods S, Rehm BH. Pseudomonas aeruginosa Lifestyle: A Paradigm for Adaptation, Survival, and Persistence. Front Cell Infect Microbiol. 2017;7:39.
40. Wiersinga WJ, van der Poll T, White NJ, Day NP, Peacock SJ. Melioidosis: insights into the pathogenicity of Burkholderia pseudomallei. Nat Rev Microbiol. 2006;4(4):272-82.
41. dos Santos PA, Pereira AC, Ferreira AF, de Mattos Alves MA, Rosa AC, Freitas-Almeida AC. Adhesion, invasion, intracellular survival and cytotoxic activity of strains of Aeromonas spp. in HEp-2, Caco-2 and T-84 cell lines. Antonie Van Leeuwenhoek. 2015;107(5):1225-36.
42. Rasmussen-Ivey CR, Figueras MJ, McGarey D, Liles MR. Virulence Factors of Aeromonas hydrophila: In the Wake of Reclassification. Front Microbiol. 2016;7:1337.
43. Tamura M, Ajayi T, Allmond LR, Moriyama K, Wiener-Kronish JP, Sawa T. Lysophospholipase A activity of Pseudomonas aeruginosa type III secretory toxin ExoU. Biochem Biophys Res Commun. 2004;316(2):323-31.
44. de Lima CD, Calegari-Silva TC, Pereira RM, Santos SA, Lopes UG, Plotkowski MC, et al. ExoU activates NF-kappaB and increases IL-8/KC secretion during Pseudomonas aeruginosa infection. PLoS One. 2012;7(7):e41772.
45. Alberti-Segui C, Goeden KR, Higgins DE. Differential function of Listeria monocytogenes listeriolysin O and phospholipases C in vacuolar dissolution following cell-to-cell spread. Cell Microbiol. 2007;9(1):179-95.
46. Sohlenkamp C, Geiger O. Bacterial membrane lipids: diversity in structures and pathways. FEMS Microbiol Rev. 2016;40(1):133-59.
47. Lemmon MA. Membrane recognition by phospholipid-binding domains. Nat Rev Mol Cell Biol. 2008;9(2):99-111.
48. Watt SA, Kular G, Fleming IN, Downes CP, Lucocq JM. Subcellular localization of phosphatidylinositol 4,5-bisphosphate using the pleckstrin homology domain of phospholipase C delta1. Biochem J. 2002;363(Pt 3):657-66.
49. Shewan A, Eastburn DJ, Mostov K. Phosphoinositides in cell architecture. Cold Spring Harb Perspect Biol. 2011;3(8):a004796.

Tables

749 **Table 1.** Plasmids used in this study

Name	Insert	Comments	Source
pDJSVT84	$FplA_{20-431}$	For production of FplA lipase domain; includes C-terminal His tag	Casasanta, Yoo (10)
pET28a+	-	Expression vector with T7 promoter	Novagen
pET28-AhPlAPass	$AhPlpA_{24-333}$	For production of *Aeromonas hydrophila* PlA lipase domain; includes C-terminal His tag	This study
pET28-AhPlAPass S67A D213N	$AhPlpA_{24-333}$	For production of catalytically inactive *Aeromonas hydrophila* PlA lipase domain; includes C-terminal His tag	This study
pET28-BpPlAPass	$BpPlA_{37-496}$	For production of *Burkholderia pseudomallei* PlA lipase domain; includes C-terminal His tag	This study
pET28-BpPlAPass S230A D378N	$BpPlA_{37-496}$	For production of catalytically inactive *Burkholderia pseudomallei* PlA lipase domain; includes C-terminal His tag	This study
pET28-BpPlAPassΔN	$BpPlA_{190-496}$	For production of *Burkholderia pseudomallei* PlA lipase domain lacking N-terminal extension; includes C-terminal His tag	This study
pET28-PlpDPass	$PlpD_{19-331}$	For production of PlpD lipase domain; includes C-terminal His tag	This study
pET28-PlpDPass I253A M256D	$PlpD_{19-331}$	For production of PlpD lipase with mutations in dimerization interface; includes C-terminal His tag	This study
pET28-PlpDPass M294E	$PlpD_{19-331}$	For production of PlpD lipase with mutation in dimerization interface; includes C-terminal His tag	This study
pET28-PlpDPass S60A D207N	$PlpD_{19-331}$	For production of catalytically inactive PlpD lipase domain; includes C-terminal His tag	This study
pET28-RsPlAPass	$RsPlA_{31-352}$	For production of *Ralstonia solanacearum* PlA lipase domain; includes C-terminal His tag	This study
pET28-RsPlAPass S85A D231N	$RsPlA_{31-352}$	For production of catalytically inactive *Ralstonia solanacearum* PlA lipase domain; includes C-terminal His tag	This study
pET28-RsPlAPassΔN	$RsPlA_{48-352}$	For production of *Ralstonia solanacearum* PlA lipase domain lacking N-terminal extension; includes C-terminal His tag	This study
pET28-VcPlAPass	$VcPlA_{22-339}$	For production of *Vibrio cholerae* PlA lipase domain; includes C-terminal His tag	This study

Table 2. Comparison of the enzymatic efficiency of all tested PlAs at pH 9 and at optimal temperatures. Shown are the Michaelis-Menten Kinetics using the graphing and data analysis software from OriginLab (Massachusetts, USA). ND=Not detectable.

Passenger	Tmp. (^{0}C)	k_{cat} (s^{-1})	K_m (µM)	k_{cat}/K_m (s^{-1} M^{-1})
PlpD$_{19-331}$	37	0.3 ± 0.04	166 ± 44	$1.8 \times 10^3 \pm 0.5 \times 10^3$
PlpD$_{19-331}$ S60A D207N	37	ND	ND	ND
AhPlA$_{24-333}$	25	10.6±1.1	120±25	$8.8 \times 10^4 \pm 2 \times 10^4$
AhPlA$_{24-333}$ S67A D213N	25	0.005 ± 0.003	27 ± 50	$1.8 \times 10^2 \pm 3.6 \times 10^2$
BpPlA$_{37-496}$	37	21.2 ± 1.9	31 ± 9	$6.9 \times 10^5 \pm 2 \times 10^5$
BpPlA$_{37-496}$ S230A D378N	37	ND	ND	ND
BpPlA$_{190-496}$	37	12 ± 1	47 ± 10	$2.6 \times 10^5 \pm 0.6 \times 10^5$
RsPlA$_{31-352}$	25	0.5 ± 0.04	62 ±13	$7.9 \times 10^3 \pm 1.8 \times 10^3$
RsPlA$_{31-352}$ S89A D231N	25	ND	ND	ND
RsPlA$_{48-352}$	25	0.1 ± 0.005	34 ± 6	$2.8 \times 10^3 \pm 0.5 \times 10^3$
FplA$_{20-431}$ *	25	55 ± 4	19.6 ± 5	$2.8 \times 10^6 \pm 0.7 \times 10^6$

***Casasanta et al., 2017**

Table 3. Estimated molecular weight of all tested PlAs based on the retention time of SEC. The MW of the monomeric proteins are shown for comparative reason and were calculated in

Protparam based on the respective amino acid sequences. The deletion of the N-terminal extension is indicated as ΔN. The reducing agent DTT was added at 10 mM in the case of the full length passenger of BpPlA due to the presence of a cysteine in the N-terminal extension of this protein.

Protein	**Est.MW [kDa]**	**Monomer [kDa]**
PlpD19-331	69	35
PlpD19-331 S60A D207N	88	35
PlpD19-331 M249E	35	-
PlpD19-331 I253A M256D	35	-
AhPlA$_{24-333}$	62	34
AhPlA$_{24-333}$ S67A D213N	61	34
BpPlA$_{37-496}$ (+DTT)	191	47
BpPlA$_{37-496}$ S230A D378N (+DTT)	178	47
BpPlA$_{190-496}$ ΔN	60	33
RsPlA$_{31-352}$	65	35
RsPlA$_{31-352}$ S89A D231N	64	35
RsPlA$_{48-352}$ pass ΔN	63	35
FplA$_{20-431}$ *	83	47

***Casasanta et al., 2017**

Table 4. Estimated molecular weight of the PlpD dimer and monomers based on the retention time of SEC. The MW of the monomeric PlpD is shown for comparative reason and was calculated in Protparam based on the respective amino acid sequence.

Protein	**Est. MW [kDa]**	**Est. MW Monomer [kDa]**
PlpD$_{19\text{-}331}$	69	35
PlpD$_{19\text{-}331}$ M249E	35	-
PlpD$_{19\text{-}331}$ I253A M256D	35	-

Table 5. Comparison of the enzymatic efficiency of the PlpD dimer and monomers at different temperatures and at pH 9. Shown are the Michaelis-Menten Kinetics using the graphing and data analysis software from OriginLab (Massachusetts, USA). ND=Not detectable.

	Tmp. (^{0}C)	**k_{cat} (s^{-1})**	**K_m (µM)**	**k_{cat}/K_m (s^{-1} M^{-1})**
PaPlpD$_{19\text{-}331}$	25	0.07 ± 0.01	51 ± 21	1.3 x 10^3 ± 0.6 x 10^3
PaPlpD$_{19\text{-}331}$	37	0.3 ± 0.04	166 ± 44	1.8 x 10^3 ± 0.5 x 10^3
PaPlpD$_{19\text{-}331}$	45	0.4 ± 0.1	186 ± 71	2.2 x 10^3 ± 1 x 10^3
PaPlpD$_{19\text{-}331}$ M249E	25	0.08 ± 0.01	37 ± 14	2.2 x 10^3 ± 0.9 x 10^3
PaPlpD$_{19\text{-}331}$ M249E	37	0.09 ± 0.01	66 ±21	1.4 x 10^3 ± 0.5 x 10^3

PaPlpD$_{19\text{-}331}$ M249E	45	0.01 ± 0.01	118 ± 310	94 ± 2.8 x 10^2
PaPlpD$_{19\text{-}331}$ I253A M256D	25	0.06 ± 0.006	40 ± 11	1.4 x 10^3 ± 0.4 x 10^3
PaPlpD$_{19\text{-}331}$ I253A M256D	37	0.09 ± 0.005	104 ± 13	8.6 x 10^2 ± 1.2 x 10^2
PaPlpD$_{19\text{-}331}$ I253A M256D	45	ND	ND	ND

Figure legends

Figure 1. Structure and sequence analysis of the lipase domains of PlpD and its homologs.

A) Structure of PlpD. The two monomers of the homodimeric protein are shown in magenta and blue in cartoon representation. The flexible lid, not visible in the crystal structure, has been drawn with a dashed lined. The active site residues are shown in stick representation (S60 in yellow and D207 in green). The figure was prepared using PyMOL (Schrödinger) based on the PlpD crystal structure (PDB ID: 5FYA).

B) Alignment of selected PlpD homologs. Predicted secondary structure elements are in blue (β-strands) or pink (α-helices); the intensity of the color refers to the strength of the prediction. Predicted signal peptides are underlined. The catalytic residues are highlighted in red. The small residues forming the oxyanion hole are indicated in orange. The position of the flexible lid is shown by a dashed yellow line and the position of the putative linker by a dashed brown line. GenBank accession numbers for the sequences are AAG06727 (PlpD), AGM45846 (AhPlA),

ABA53592 (BpPlA), KER53746 (BfPlA), AAQ60385 (CvPlA), AAL93819 (FplA), AFJ59299 (PfPlA), EAP74568 (RsPlA), AAN53510 (SoPlA), and AAF93770 (VcPlA).

Figure 2. Lipolytic activity of all tested PlAs. A) Michaelis-Menten Kinetics based on fluorescence produced by the hydrolysis of the artificial substrate 4-MuH. B) Phospholipase A1 (left) and A2 (right) activity using the PLA1 and PLA2-specific substrates PED-A1 and BODIPY PC-A2, respectively. Error bars denote standard deviations. Ctrl: Phospholipase A1/A2 (ThermoFisher). ND=Not detectable.

Figure 3. Lipid binding assays. Strips with bound lipids (indicated in the Figure) were overlaid with PlAs and then detected using an anti-His tag antibody. Catalytically inactive mutants of the PlAs were used so as not to damage the lipids, but results were comparable to catalytically active protein (Figure S4). The lipids impregnated on the left side of the strip are noted on the left in the figure, and those on the right-hand side of the strip to the right in the figure.

Figure 4. Specific lipid hydrolysis by PlAs. Lipids were incubated with PlAs for 24 h. Detection of lipid digestion are shown by TLC. Lipids incubated in the absence of any PLA were used as negative control. Solvent systems used as mobile phase are mentioned below individual figures. A) Phosphatidylethanolamine (PE). B) Phosphatidylserine (PS). C) Phosphatidylinositol 4-phosphate (PI(4)P). D) Soy lipid extract.

Figure 5. Oligomerization of PlA passengers. A) Alignment of the dimerization interface of the different PlAs. B) SDS-PAGE of all tested PlAs in the presence and absence of the amine-amine cross-linker BS3. C) SEC of *P. aeruginosa* PlpD passenger as well as its homologs from *A.*

hydrophila, *R. solanacearum* and *B. pseudomallei*. Wt passengers are shown in red, the truncated passenger of *B. pseudomallei* with deletion of the N-terminal extension is shown in blue and the molecular weight standards (Vitamin B12 [1.35 kDa]; Myoglobin (horse) [17 kDa]; Ovalbumin (chicken) [44 kDa]; γ-globulin (bovine) [158 kDa]; Thyroglobulin (bovine) [670 kDa]; Biorad) are shown in grey. Signal data may have been enhanced for data presentation by factor x as indicated in [] behind the respective protein. D) Comparative overview of the multimerization status of the tested PlAs based on SEC. Indicated in white are the estimated MWs of the monomeric proteins, indicated in red are the estimated MWs based on SEC data gathered in this study, indicated with dotted lines are the expected MWs of the dimeric proteins and indicated in shades of grey are the expected MWs of the BpPlA dimer, trimer and tetramer (dimer-dimer). Calculated and expected MWs are shown in Table 3.

Figure 6. Mutation of the dimerization interface of the PlpD homodimer leads to disruption of the homodimer. A) Dimerization interface of two neighboring molecules in the homodimer of PlpD (PDB: 5FYA). B) SEC of the PlpD dimer (red) and its monomeric forms, PlpD M249E (blue) and PlpD I253E M256D (green). Shown in grey are the molecular weight standards (Vitamin B12 [1.35 kDa]; Myoglobin (horse) [17 kDa]; Ovalbumin (chicken) [44 kDa]; γ-globulin (bovine) [158 kDa]; Thyroglobulin (bovine) [670 kDa]; Biorad). C) Cross-linking of dimeric PlpD using the amine-amine cross-linker BS3.

Figure 7. Homodimer-formation by PlpD is not necessary for activity. A) Michaelis-Menten kinetics of the PlpD dimer and monomers (PlpD M249E and PlpD I253A M256D) at 25^0C, 37^0C

and 45^0C. The working concentration of PlpD, PlpD M249E and PlpD I253A M256D were 1 µM, 100 nM and 100 nM, respectively. B) Phospholipase activity 1 of the PlpD dimer compared to the monomers. See legend of Figure 2 for full description.

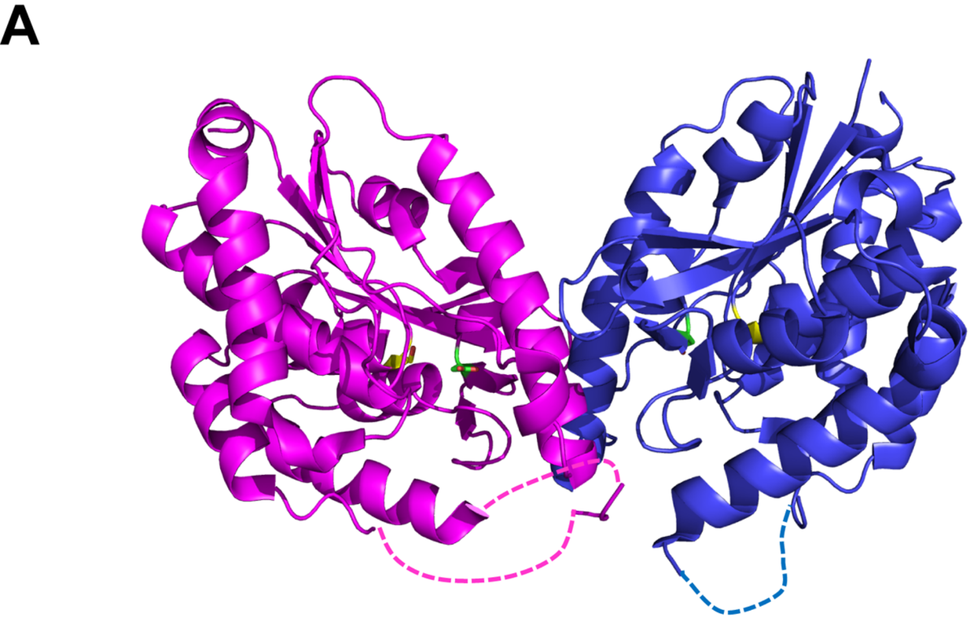
A

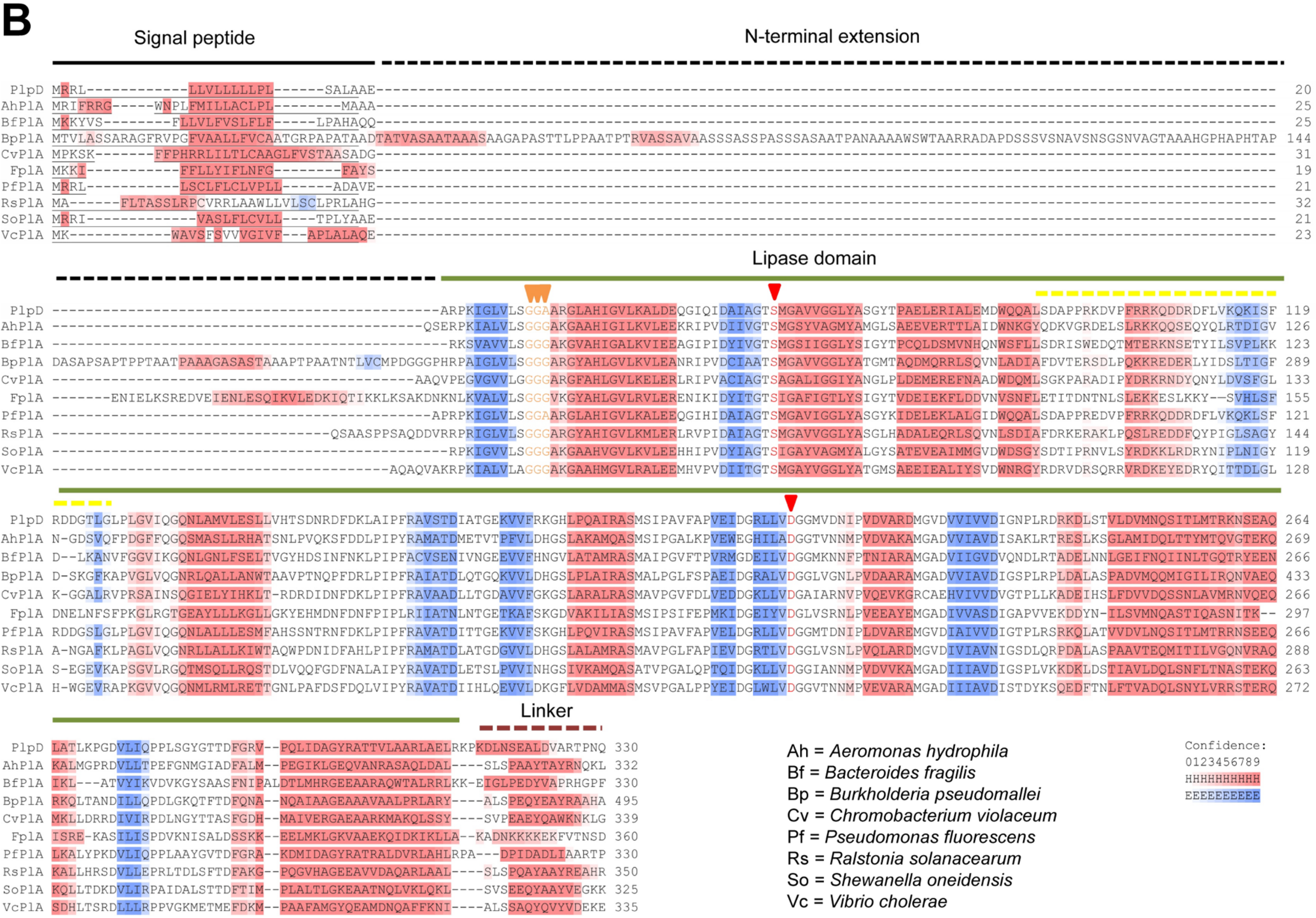
B
Signal peptide
N-terminal extension
Lipase domain
Linker
PlpD
AhPlA
BfPlA
BpPlA
CvPlA
FpIA
PfPlA
RsPlA
SoPlA
VcPlA
Ah = Aeromonas hydrophila
Bf = Bacteroides fragilis
Bp = Burkholderia pseudomallei
Cv = Chromobacterium violaceum
Pf = Pseudomonas fluorescens
Rs = Ralstonia solanacearum
So = Shewanella oneidensis
Vc = Vibrio cholerae
Confidence:
0123456789
HHHHHHHHHH
EEEEEEEEEE

A

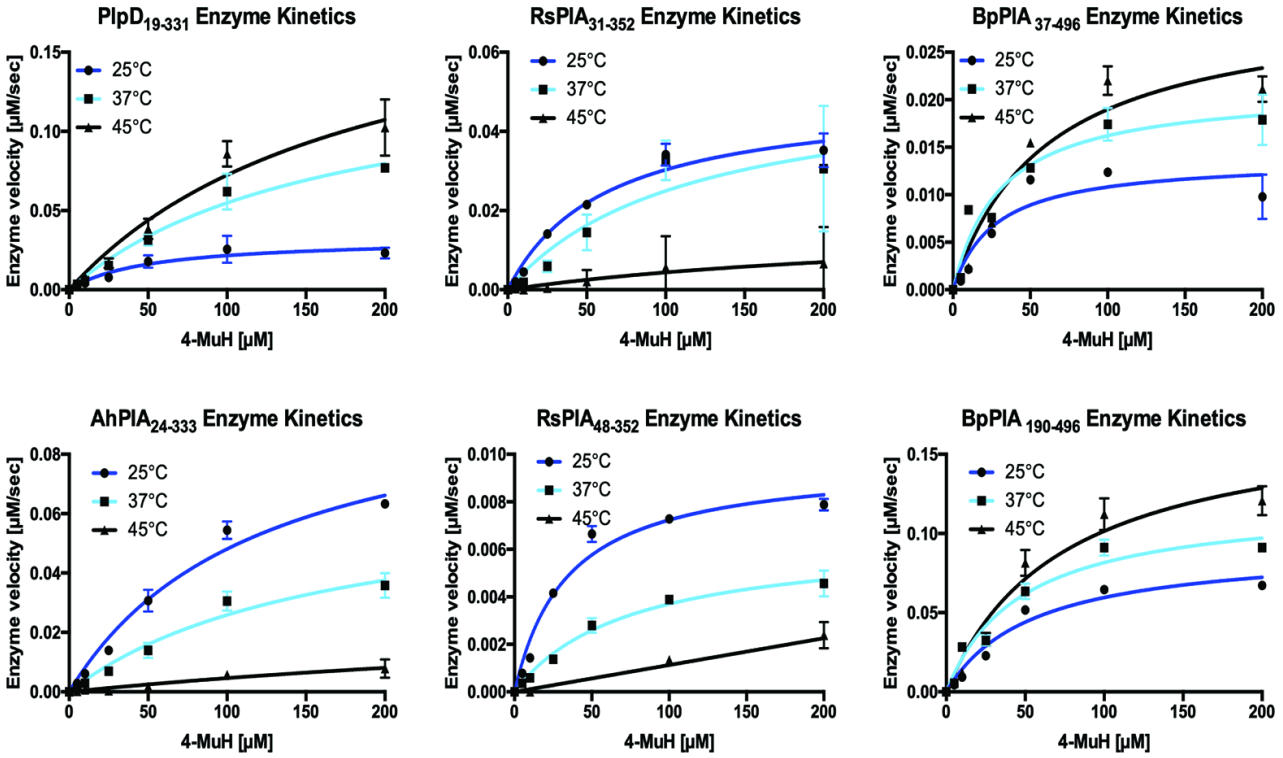
PlpD19-331 Enzyme Kinetics
RsPlA31-352 Enzyme Kinetics
BpPlA 37-496 Enzyme Kinetics
AhPlA24-333 Enzyme Kinetics
RsPlA48-352 Enzyme Kinetics
BpPlA 190-496 Enzyme Kinetics
25°C
37°C
45°C
Enzyme velocity [µM/sec]
4-MuH [µM]

B

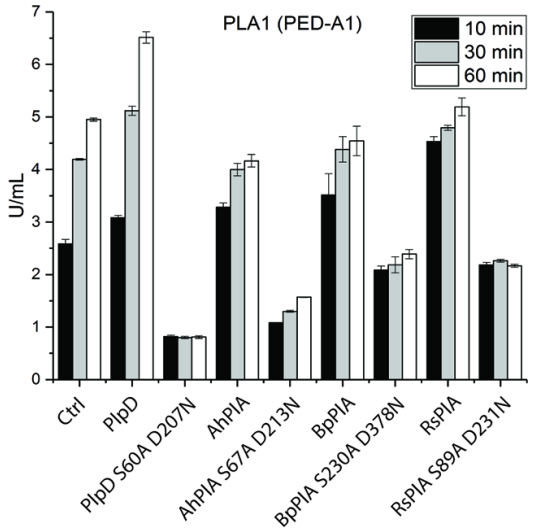
PLA1 (PED-A1)
10 min
30 min
60 min
U/mL
Ctrl
PlpD
PlpD S60A D207N
AhPlA
AhPlA S67A D213N
BpPlA
BpPlA S230A D378N
RsPlA
RsPlA S89A D231N

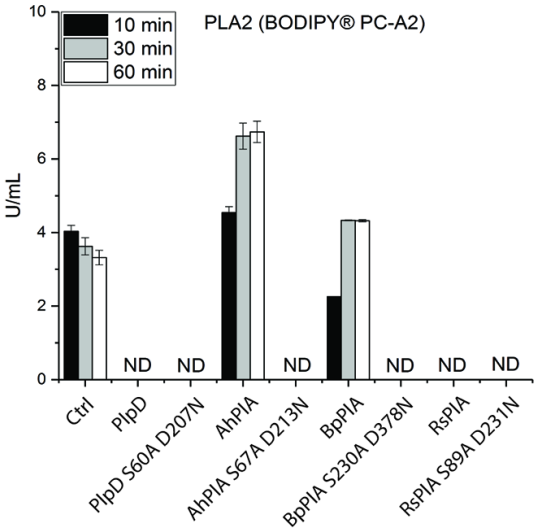
PLA2 (BODIPY® PC-A2)
10 min
30 min
60 min
U/mL
ND
Ctrl
PlpD
PlpD S60A D207N
AhPlA
AhPlA S67A D213N
BpPlA
BpPlA S230A D378N
RsPlA
RsPlA S89A D231N

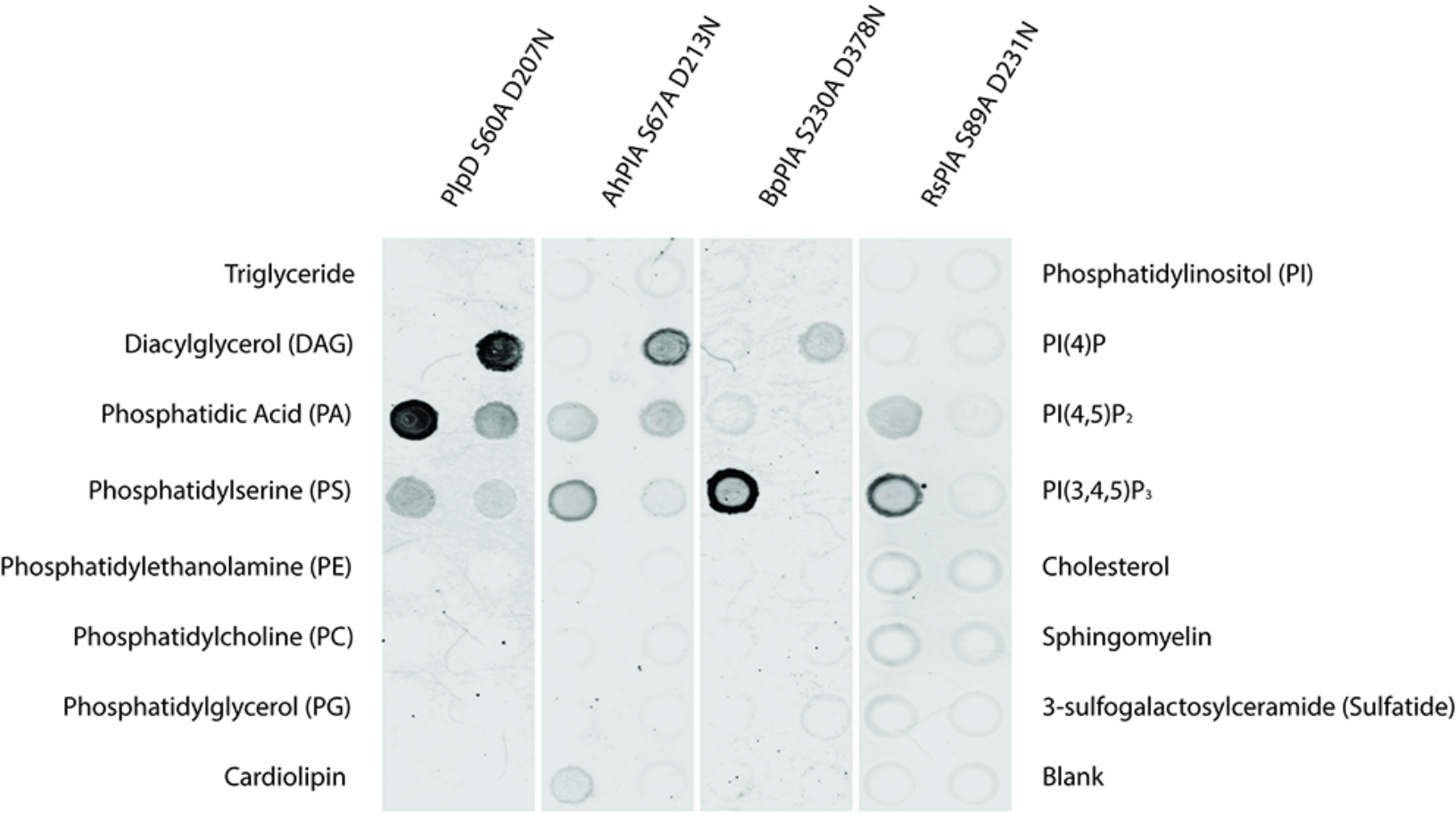
PlpD S60A D207N
AhPlA S67A D213N
BpPlA S230A D378N
RsPlA S89A D231N
Triglyceride
Diacylglycerol (DAG)
Phosphatidic Acid (PA)
Phosphatidylserine (PS)
Phosphatidylethanolamine (PE)
Phosphatidylcholine (PC)
Phosphatidylglycerol (PG)
Cardiolipin
Phosphatidylinositol (PI)
PI(4)P
PI(4,5)P2
PI(3,4,5)P3
Cholesterol
Sphingomyelin
3-sulfogalactosylceramide (Sulfatide)
Blank

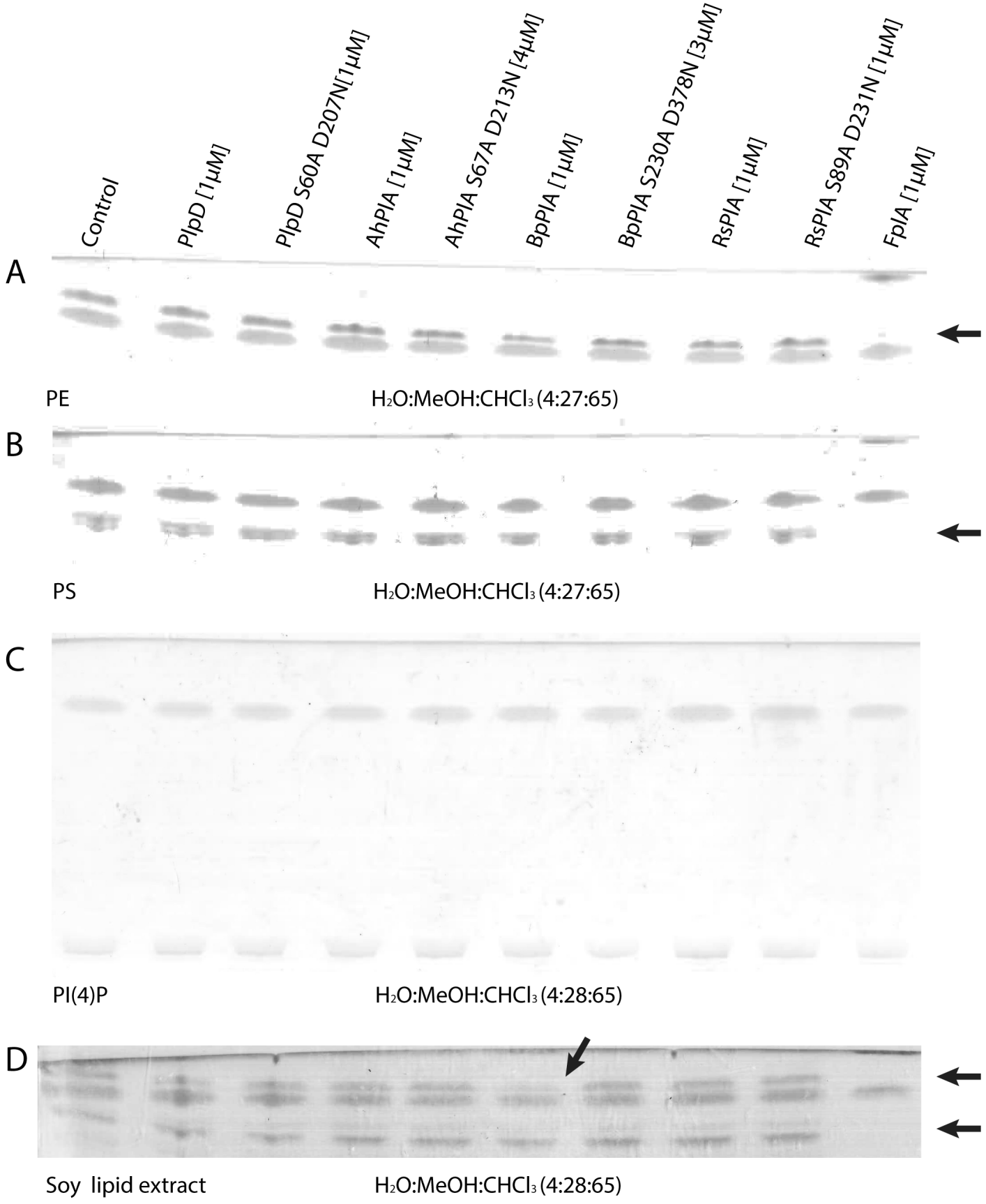
Control
PlpD [1μM]
PlpD S60A D207N[1μM]
AhPlA [1μM]
AhPlA S67A D213N [4μM]
BpPlA [1μM]
BpPlA S230A D378N [3μM]
RsPlA [1μM]
RsPlA S89A D231N [1μM]
FplA [1μM]
A
PE
H2O:MeOH:CHCl3 (4:27:65)
B
PS
H2O:MeOH:CHCl3 (4:27:65)
C
PI(4)P
H2O:MeOH:CHCl3 (4:28:65)
D
Soy lipid extract
H2O:MeOH:CHCl3 (4:28:65)

A

```
PlpD   237 RDRKDLSTVLDVMNQSITLMTRKNSEAQLATLK 269
AhPlA  243 RTRESLKSGLAMIDQLTTYMTQVGTEKQKALMG 275
BpPlA  405 RPLDALASPADVMQQMIGILIRQNVAEQRKQLT 437
FplA   273 VEKDDYN-ILSVMNQASTIQASNITKISREKA- 303
RsPlA  261 QRPDALASPAAVTEQMITILVGQNVRAQKALLH 293
VcPlA  245 KSQEDFTNLFTVADQLSNYLVRRS      DHLT 277

Confidence:
0123456789
HHHHHHHHHH
EEEEEEEEEE
```

B

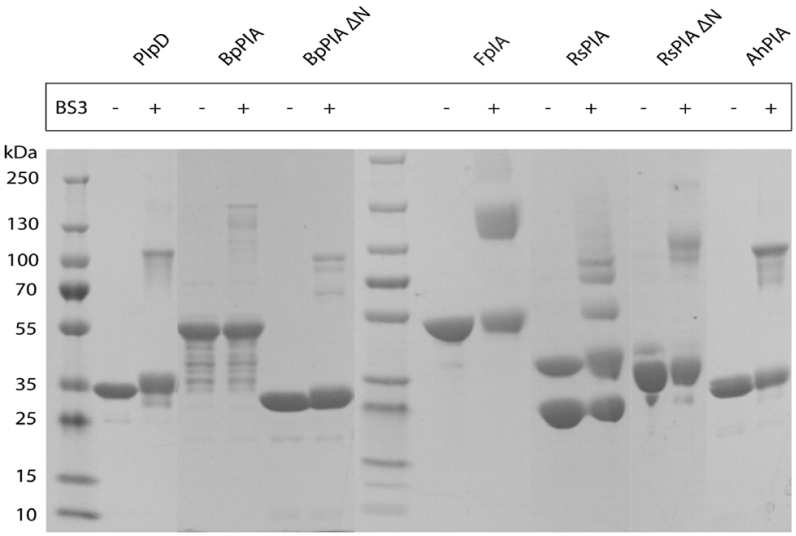

C

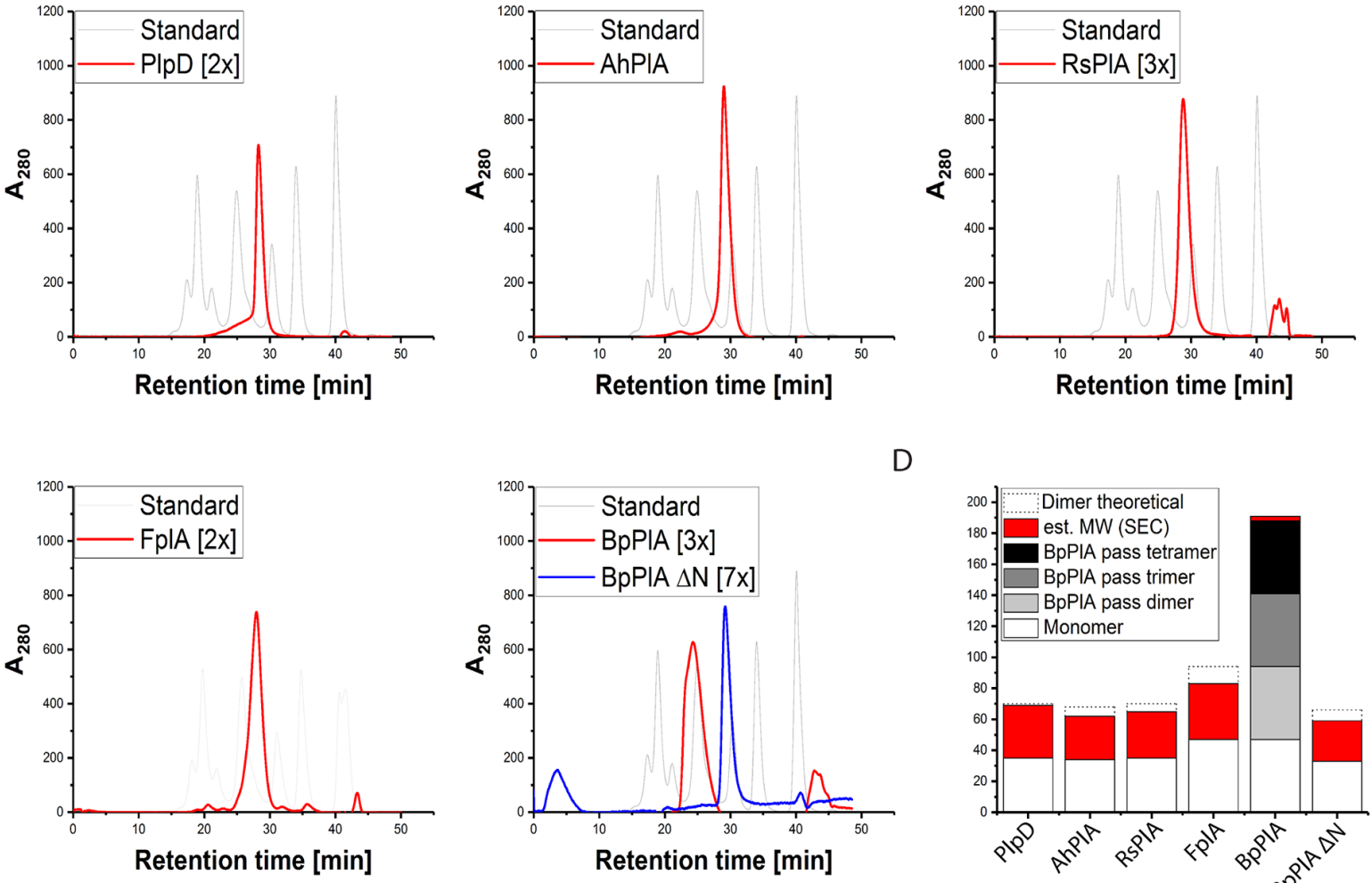

D

A

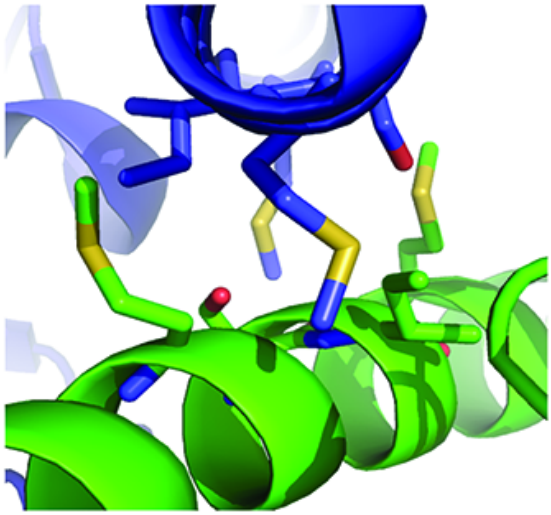

B

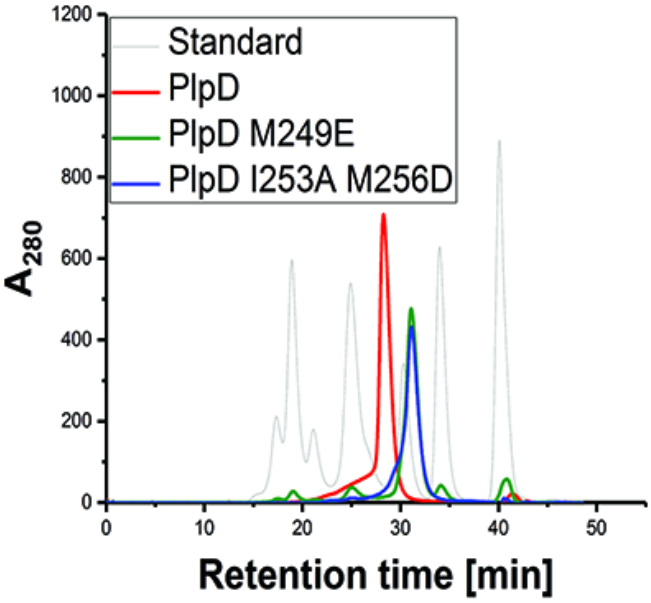
Standard
PlpD
PlpD M249E
PlpD I253A M256D
A_{280}
Retention time [min]
0
200
400
600
800
1000
1200
0
10
20
30
40
50

C

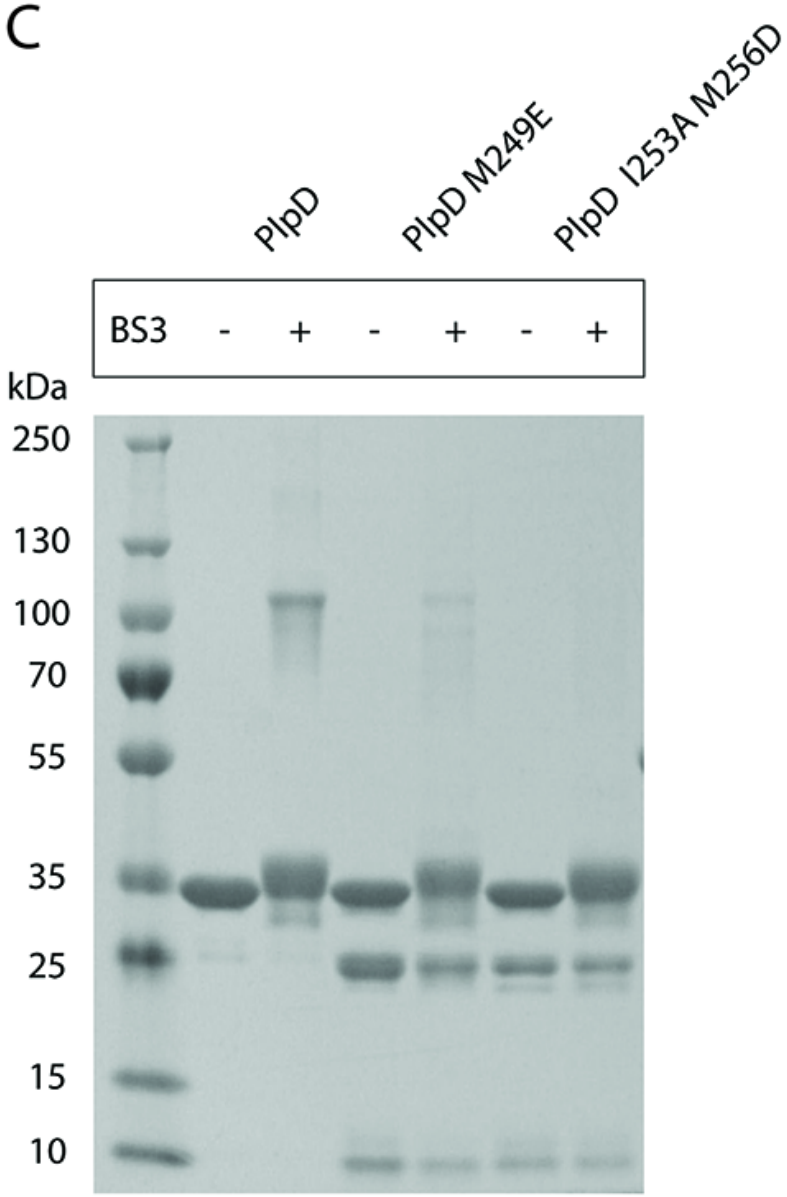
PlpD
PlpD M249E
PlpD I253A M256D
BS3 - + - + - +
kDa
250
130
100
70
55
35
25
15
10

A

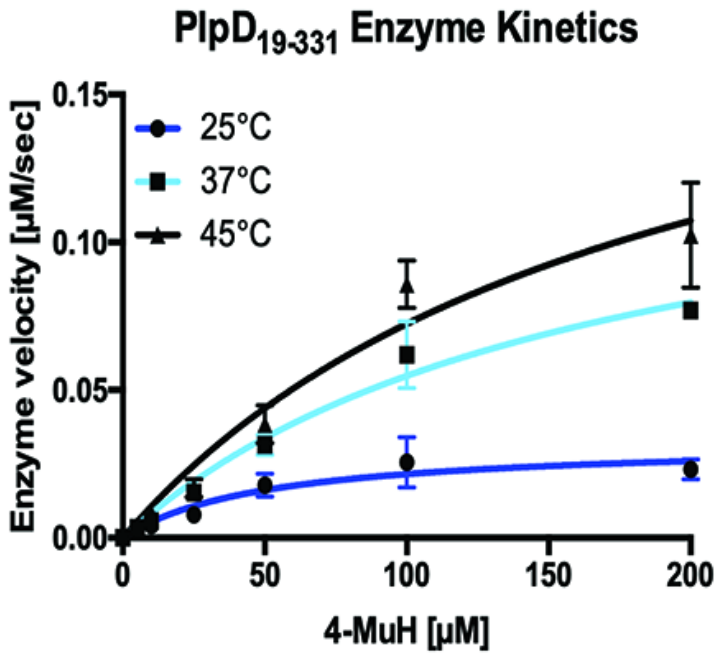
PlpD19-331 Enzyme Kinetics
Enzyme velocity [µM/sec]
0.15
0.10
0.05
0.00
25°C
37°C
45°C
0
50
100
150
200
4-MuH [µM]

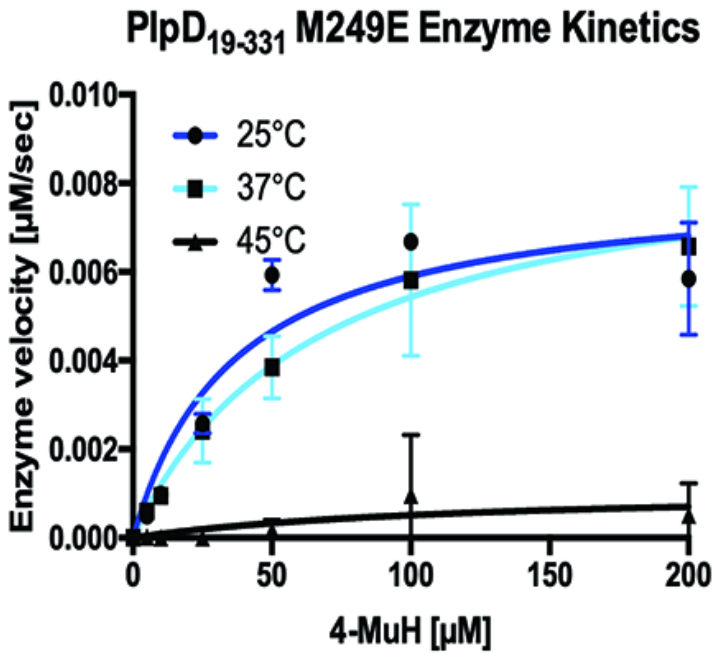
PlpD19-331 M249E Enzyme Kinetics
Enzyme velocity [µM/sec]
0.010
0.008
0.006
0.004
0.002
0.000
25°C
37°C
45°C
0
50
100
150
200
4-MuH [µM]

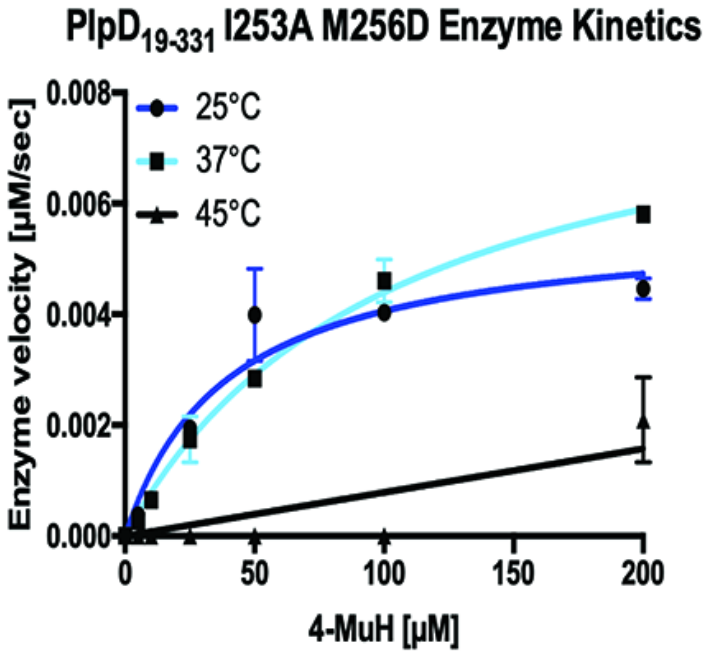
PlpD19-331 I253A M256D Enzyme Kinetics
Enzyme velocity [µM/sec]
0.008
0.006
0.004
0.002
0.000
25°C
37°C
45°C
0
50
100
150
200
4-MuH [µM]

B

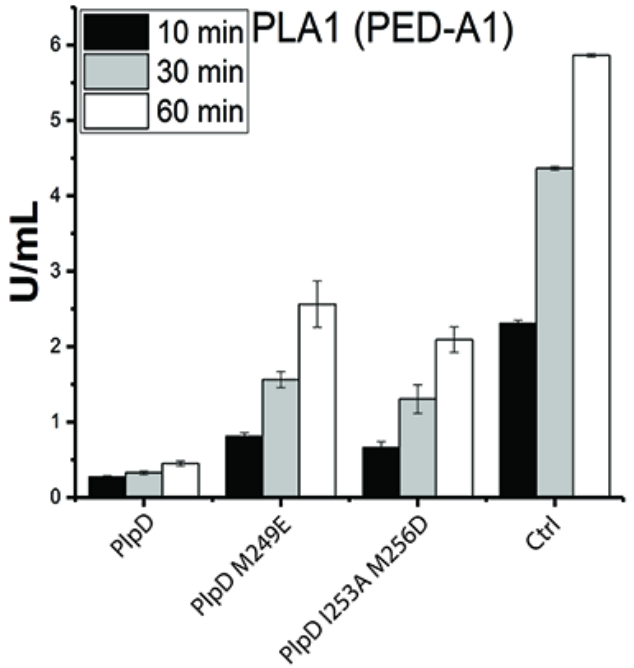
PLA1 (PED-A1)
10 min
30 min
60 min
U/mL
0
1
2
3
4
5
6
PlpD
PlpD M249E
PlpD I253A M256D
Ctrl

Comparison of type 5d autotransporter phospholipases demonstrates a correlation between high activity and intracellular pathogenic lifestyle

Thomas Trunk[1], Michael A. Casasanta[2], Christopher C. Yoo[2], Daniel J. Slade[2], Jack C. Leo[1,3*]

[1]Department of Bioscience, University of Oslo, Oslo 0316, Norway

[2]Department of Biochemistry, Virginia Polytechnic Institute and State University, Blacksburg, Virginia, VA 24061, USA

[3]Present address: Department of Biosciences, School of Science and Technology, Nottingham Trent University, Nottingham NG1 4FQ, United Kingdom

[*]corresponding author: Jack C. Leo, Blindern 31, 0371 Oslo, Norway, tel.: +47-22859027, j.c.leo@ibv.uio.no

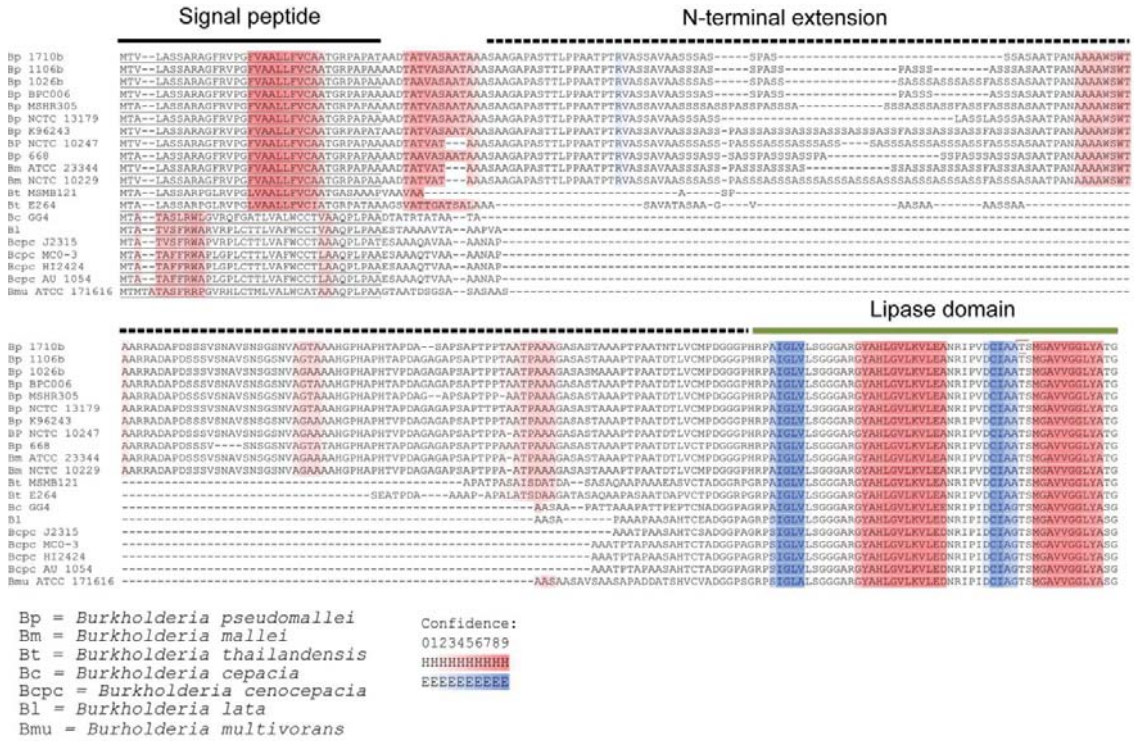

Figure S1. PlAs *Burkholderia* sp. have an N-terminal extension

Alignment of PlA passenger N-terminal sequences from *Burkholderia* strains. All *Bulkholderiae* have an N-terminal extension, but only PlAs from *B. pseudomallei* and *B. mallei* have one longer than ~40 residues. Genbank accession numbers for the sequences are ABA53592 (Bp 1710b), WP_011857657 (Bp 1106b), AFI68957 (Bp 1026b), AFR18824 (Bp BPC006), AGR68910 (Bp MSHR305), AGZ32405 (Bp NCTC 13179), YP_110653 (Bp K96243), YP_001078772 (Bp NCTC 10247), ABN86253 (Bp 668), YP_105527 (Bm ATCC 23344), WP_011831963 (Bm NCTC 10229), AGK50760 (Bt MSMB121), AIP28840 (Bt E264), AFQ49895 (Bc GG4), ABB10869 (Bl), CAR56030 (Bcpc J2315), ACA94478 (Bcpc MC0-3), ABK11671 (Bcpc HI2424), ABF78326 (Bcpc AU 1054), and ABX17368 (Bmu ATCC 171616).

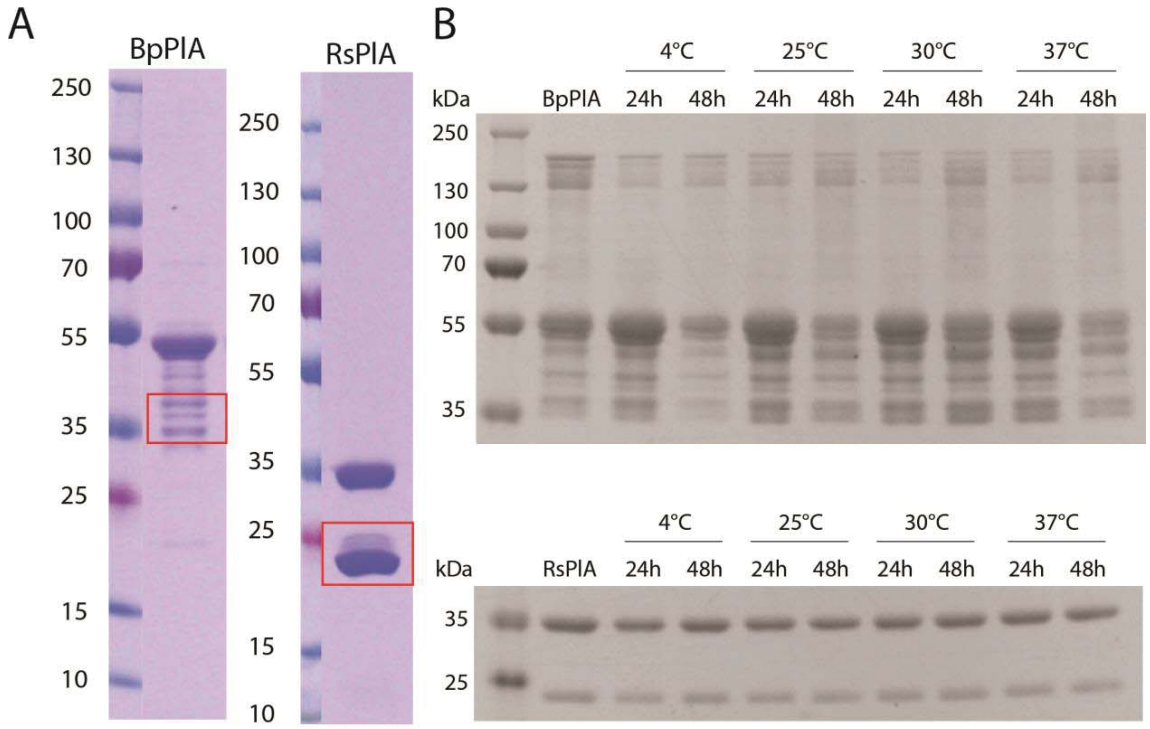

C

Peptides detected in MS shown in red

BpPlpD proteolysed fragment from MS

MADTATVASAATAAASAAGAPASTTLPPAATPTRVASSAVAASSSASSPASSSASAATPANAAAAWSWTAARRAD
APDSSSVSNAVSNSGSNVAGTAAAHGPHAPHTAPDASAPSAPTPPTAATPAAAGASASTAAAPTPAATNTLVCMP
DGGGPHRPAIGLVLSGGGARGYAHLGVLKVLEANRIPVDCIAATSMGAVVGGLYATGMTAQDMQRRLSQVNLADI
AFDVTERSDLPQKKREDERLYIDSLTIGFDSKGFKAPVGLVQGNRLQALLANWTAAVPTNQPFDRLPIPFRAIAT
DLQTGQKVVLDHGSLPLAIRASMALPGLFSPAEIDGRALVDGGLVGNLPVDAARAMGADVVIAVDIGSPLRPLDA
LASPADVMQQMIGILIRQNVAEQRKQLTANDILLQPDLGKQTFTDFQNANQAIAAGEAAAVAALPRLARYALSPE
QYEAYRAAHARHHHHHH

RsPlpD proteolysed fragment from MS
MHGQSAASPPSAQDDVRRPRIGLVLSGGGARGYAHIGVLKMLERLRVPIDAIAGTAMGAVVGGLYASGLHADALE
QRLSQVNLSDIAFDRKERAKLPQSLREDDFQYPIGLSAGYANGAFKLPAGLVQGNRLLALLKIWTAQWPDNIDFA
HLPIPFRAMATDLATGDGVVLDHGSLALAMRASMAVPGLFAPIEVDGRTLVNGGLVSNLPVQLARDMGVDIVIAV
NIGSDLQRPDALASPAAVTEQMITILVGQNVRAQKALLHRSDVLLEPRLTDLSFTDFAKGPQGVHAGEEAVVDAQ
ARLAALSLSPQAYAAYREAHRPQHHHHHHH

Figure S2. BpPlA and RsPlA degradation product

A) Degradation of PlAs noticed during protein purification in the case of BpPlA (left) and RsPlA (right) B) Degradation of RsPlA and BpPlA at different time points and different temperatures after sample defrosting. Freshly defrosted sample was used as control. C) Low

molecular weight bands are degradation products of BpPlA and RsPlA, respectively. Confirmed by mass spectrometric analysis.

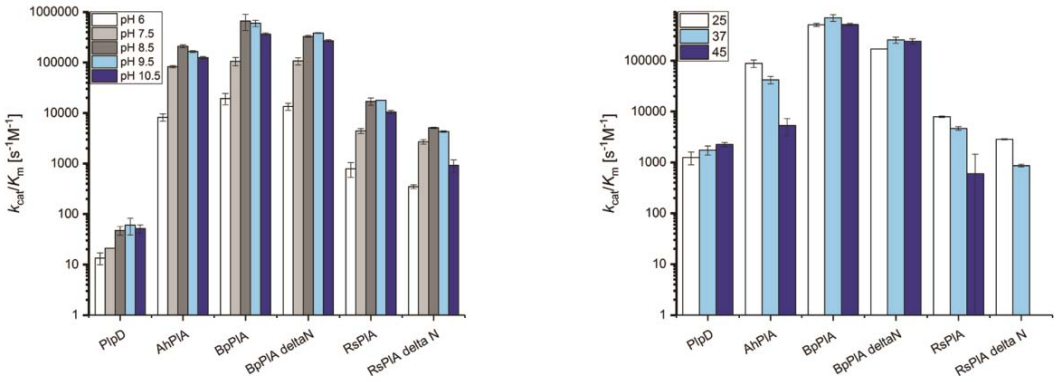

Figure S3. pH and temperature optima of target PlAs

pH (left) and temperature range (right) of target PlAs based on Michaelis-Menten kinetics using the artificial lipid substrate 4-MuH.

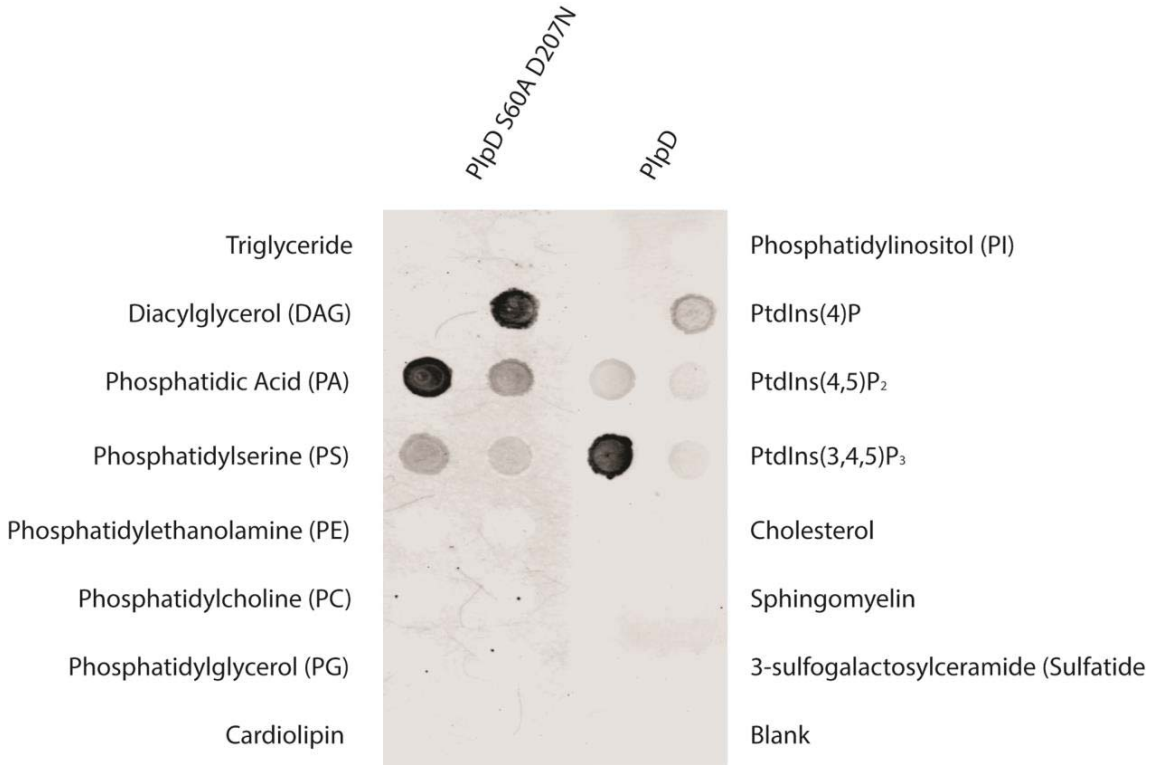

Figure S4. Comparison of lipid binding between PlpD and PlpD S60A D207N

Lipid binding assays. Mutation of the catalytic dyad has no major effect on lipid binding. Strips with bound lipids (indicated in the Figure) were overlaid with wildtype PlpD (right) or inactive PlpD (left) and then detected using an anti-His tag antibody. The lipids impregnated on the left side of the strip are noted on the left in the figure, and those on the right-hand side of the strip to the right in the figure.

A

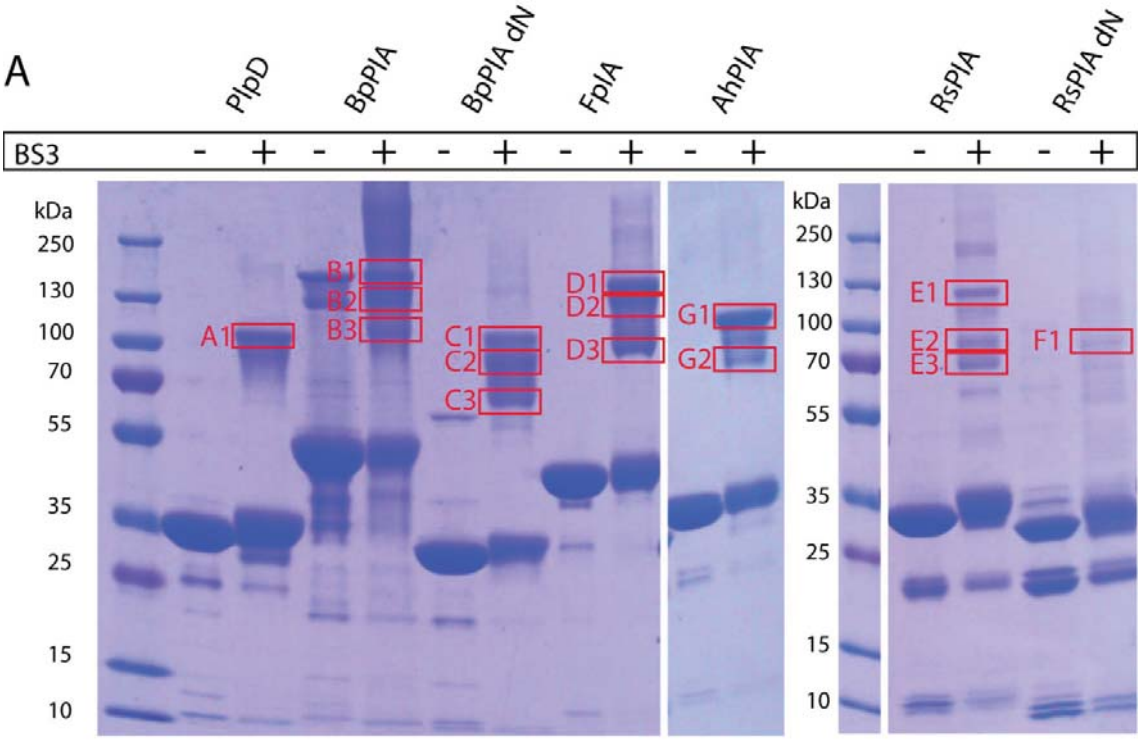

B

A1

A1 (100%), 34 672,5 Da
Pseudomonas aeruginosa PlpD | Trunk T
19 exclusive unique peptides, 37 exclusive unique spectra, 297 total spectra, 194/320 amino acids (61% coverage)

```
MAEARPKIGL  VLSGGAARGL  AHIGVLKALD  EQGIQIDAIA  GTSMGAVVGG
LYASGYTPAE  LERIALEMDW  QQALSDAPPR  KDVPFRRKQD  DRDFLVKQKI
SFRDDGTLGL  PLGVIQGQNL  AMVLESLLVH  TSDNRDFDKL  AIPFRAVSTD
IATGEKVVFR  KGHLPQAIRA  SMSIPAVFAP  VEIDGRLLVD  GGMVDNIPVD
VARDMGVDVV  IVVDIGNPLR  DRKDLSTVLD  VMNQSITLMT  RKNSEAQLAT
LKPGDVLIQP  PLSGYGTTDF  GRVPQLIDAG  YRATTVLAAR  LAELRKPKDL
NSEALDVART  PNQRHHHHHH
```

B1

B1-3/C1-3 (100%), 47 201,3 Da
Burkholderia pseudomallei PLA | Trunk T
17 exclusive unique peptides, 32 exclusive unique spectra, 213 total spectra, 221/467 amino acids (47% coverage)

```
MADTATVASA  ATAAASAAGA  PASTTLPPAA  TPTRVASSAV  AASSSASSPA
SSSASAATPA  NAAAAWSWTA  ARRADAPDSS  SVSNAVSNSG  SNVAGTAAAH
GPHAPHTAPD  ASAPSAPTPP  TAATPAAAGA  SASTAAAPTP  AATNTLVCMP
DGGGPHRPAI  GLVLSGGGAR  GYAHLGVLKV  LEANRIPVDC  IAATSMGAVV
GGLYATGMTA  QDMQRRLSQV  NLADIAFDVT  ERSDLPQKKR  EDERLYIDSL
TIGFDSKGFK  APVGLVQGNR  LQALLANWTA  AVPTNQPFDR  LPIPFRAIAT
DLQTGQKVVL  DHGSLPLAIR  ASMALPGLFS  PAEIDGRALV  DGGLVGNLPV
DAARAMGADV  VIAVDIGSPL  RPLDALASPA  DVMQQMIGIL  IRQNVAEQRK
QLTANDILLQ  PDLGKQTFTD  FQNANQAIAA  GEAAAVAALP  RLARYALSPE
QYEAYRAAHA  RHHHHHH
```

B2

B1-3/C1-3 (100%), 47 201,3 Da
Burkholderia pseudomallei PLA | Trunk T
17 exclusive unique peptides, 32 exclusive unique spectra, 244 total spectra, 221/467 amino acids (47% coverage)

```
MADTATVASA  ATAAASAAGA  PASTTLPPAA  TPTRVASSAV  AASSSASSPA
SSSASAATPA  NAAAAWSWTA  ARRADAPDSS  SVSNAVSNSG  SNVAGTAAAH
GPHAPHTAPD  ASAPSAPTPP  TAATPAAAGA  SASTAAAPTP  AATNTLVCMP
DGGGPHRPAI  GLVLSGGGAR  GYAHLGVLKV  LEANRIPVDC  IAATSMGAVV
GGLYATGMTA  QDMQRRLSQV  NLADIAFDVT  ERSDLPQKKR  EDERLYIDSL
TIGFDSKGFK  APVGLVQGNR  LQALLANWTA  AVPTNQPFDR  LPIPFRAIAT
DLQTGQKVVL  DHGSLPLAIR  ASMALPGLFS  PAEIDGRALV  DGGLVGNLPV
DAARAMGADV  VIAVDIGSPL  RPLDALASPA  DVMQQMIGIL  IRQNVAEQRK
QLTANDILLQ  PDLGKQTFTD  FQNANQAIAA  GEAAAVAALP  RLARYALSPE
QYEAYRAAHA  RHHHHHH
```

B3

B1-3/C1-3 (100%), 47 201,3 Da
Burkholderia pseudomallei PLA | Trunk T
13 exclusive unique peptides, 19 exclusive unique spectra, 74 total spectra, 161/467 amino acids (34% coverage)

```
MADTATVASA  ATAAASAAGA  PASTTLPPAA  TPTRVASSAV  AASSSASSPA
SSSASAATPA  NAAAAWSWTA  ARRADAPDSS  SVSNAVSNSG  SNVAGTAAAH
GPHAPHTAPD  ASAPSAPTPP  TAATPAAAGA  SASTAAAPTP  AATNTLVCMP
DGGGPHRPAI  GLVLSGGGAR  GYAHLGVLKV  LEANRIPVDC  IAATSMGAVV
GGLYATGMTA  QDMQRRLSQV  NLADIAFDVT  ERSDLPQKKR  EDERLYIDSL
TIGFDSKGFK  APVGLVQGNR  LQALLANWTA  AVPTNQPFDR  LPIPFRAIAT
DLQTGQKVVL  DHGSLPLAIR  ASMALPGLFS  PAEIDGRALV  DGGLVGNLPV
DAARAMGADV  VIAVDIGSPL  RPLDALASPA  DVMQQMIGIL  IRQNVAEQRK
QLTANDILLQ  PDLGKQTFTD  FQNANQAIAA  GEAAAVAALP  RLARYALSPE
QYEAYRAAHA  RHHHHHH
```

C1

B1-3/C1-3 (100%), 47 201,3 Da
Burkholderia pseudomallei PLA | Trunk T
13 exclusive unique peptides, 21 exclusive unique spectra, 110 total spectra, 161/467 amino acids (34% coverage)

```
MADTATVASA  ATAAASAAGA  PASTTLPPAA  TPTRVASSAV  AASSSASSPA
SSSASAATPA  NAAAAWSWTA  ARRADAPDSS  SVSNAVSNSG  SNVAGTAAAH
GPHAPHTAPD  ASAPSAPTPP  TAATPAAAGA  SASTAAAPTP  AATNTLVCMP
DGGGPHRPAI  GLVLSGGGAR  GYAHLGVLKV  LEANRIPVDC  IAATSMGAVV
GGLYATGMTA  QDMQRRLSQV  NLADIAFDVT  ERSDLPQKKR  EDERLYIDSL
TIGFDSKGFK  APVGLVQGNR  LQALLANWTA  AVPTNQPFDR  LPIPFRAIAT
DLQTGQKVVL  DHGSLPLAIR  ASMALPGLFS  PAEIDGRALV  DGGLVGNLPV
DAARAMGADV  VIAVDIGSPL  RPLDALASPA  DVMQQMIGIL  IRQNVAEQRK
QLTANDILLQ  PDLGKQTFTD  FQNANQAIAA  GEAAAVAALP  RLARYALSPE
QYEAYRAAHA  RHHHHHH
```

C2

B1-3/C1-3 (100%), 47 201,3 Da
Burkholderia pseudomallei PLA | Trunk T
14 exclusive unique peptides, 24 exclusive unique spectra, 197 total spectra, 181/467 amino acids (39% coverage)

```
MADTATVASA  ATAAASAAGA  PASTTLPPAA  TPTRVASSAV  AASSSASSPA
SSSASAATPA  NAAAAWSWTA  ARRADAPDSS  SVSNAVSNSG  SNVAGTAAAH
GPHAPHTAPD  ASAPSAPTPP  TAATPAAAGA  SASTAAAPTP  AATNTLVCMP
DGGGPHRPAI  GLVLSGGGAR  GYAHLGVLKV  LEANRIPVDC  IAATSMGAVV
GGLYATGMTA  QDMQRRLSQV  NLADIAFDVT  ERSDLPQKKR  EDERLYIDSL
TIGFDSKGFK  APVGLVQGNR  LQALLANWTA  AVPTNQPFDR  LPIPFRAIAT
DLQTGQKVVL  DHGSLPLAIR  ASMALPGLFS  PAEIDGRALV  DGGLVGNLPV
DAARAMGADV  VIAVDIGSPL  RPLDALASPA  DVMQQMIGIL  IRQNVAEQRK
QLTANDILLQ  PDLGKQTFTD  FQNANQAIAA  GEAAAVAALP  RLARYALSPE
QYEAYRAAHA  RHHHHHH
```

C3

B1-3/C1-3 (100%), 47 201,3 Da
Burkholderia pseudomallei PLA | Trunk T
18 exclusive unique peptides, 30 exclusive unique spectra, 259 total spectra, 221/467 amino acids (47% coverage)

```
MADTATVASA  ATAAASAAGA  PASTTLPPAA  TPTRVASSAV  AASSSASSPA
SSSASAATPA  NAAAAWSWTA  ARRADAPDSS  SVSNAVSNSG  SNVAGTAAAH
GPHAPHTAPD  ASAPSAPTPP  TAATPAAAGA  SASTAAAPTP  AATNTLVCMP
DGGGPHRPAI  GLVLSGGGAR  GYAHLGVLKV  LEANRIPVDC  IAATSMGAVV
GGLYATGMTA  QDMQRRLSQV  NLADIAFDVT  ERSDLPQKKR  EDERLYIDSL
TIGFDSKGFK  APVGLVQGNR  LQALLANWTA  AVPTNQPFDR  LPIPFRAIAT
DLQTGQKVVL  DHGSLPLAIR  ASMALPGLFS  PAEIDGRALV  DGGLVGNLPV
DAARAMGADV  VIAVDIGSPL  RPLDALASPA  DVMQQMIGIL  IRQNVAEQRK
QLTANDILLQ  PDLGKQTFTD  FQNANQAIAA  GEAAAVAALP  RLARYALSPE
QYEAYRAAHA  RHHHHHH
```

D1

D1-3 (100%), 46 898,9 Da
Fusobacterium nucleatum (FplA) | Trunk T
31 exclusive unique peptides, 43 exclusive unique spectra, 237 total spectra, 236/419 amino acids (56% coverage)

```
MENIELKSRE  DVEIENLESQ  IKVLEDKIQT  IKKLKSAKDN  KNLKVALVLS
GGGVKGYAHL  GVLRVLEREN  IKIDYITGTS  IGAFIGTLYS  IGYTVDEIEK
FLDDVNVSNF  LETITDNTNL  SLEKKESLKK  YSVHLSFDNE  LNFSFPKGLR
GTGEAYLLLK  GLLGKYEHMD  NFDNFPIPLR  IIATNLNTGE  TKAFSKGDVA
KILIASMSIP  SIFEPMKIDG  EIYVDGLVSR  NLPVEEAYEM  GADIVVASDI
GAPVVEKDDY  NILSVMNQAS  TIQASNITKI  SREKASILIS  PDVKNISALD
SSKKEELMKL  GKVAAEKQID  KIKLLAKADN  KKKKEKFVTN  SDAKIIINKI
EYNDKFDKNT  VIVLNDIFKG  LLNNPISKKD  IDKKIIDVYS  SKYMDKVYYT
VDNGVLYLDG  EKAHHHHHH
```

D2

D1-3 (100%), 46 898,9 Da
Fusobacterium nucleatum (FplA) | Trunk T
24 exclusive unique peptides, 31 exclusive unique spectra, 196 total spectra, 218/419 amino acids (52% coverage)

```
MENIELKSRE  DVEIENLESQ  IKVLEDKIQT  IKKLKSAKDN  KNLKVALVLS
GGGVKGYAHL  GVLRVLEREN  IKIDYITGTS  IGAFIGTLYS  IGYTVDEIEK
FLDDVNVSNF  LETITDNTNL  SLEKKESLKK  YSVHLSFDNE  LNFSFPKGLR
GTGEAYLLLK  GLLGKYEHMD  NFDNFPIPLR  IIATNLNTGE  TKAFSKGDVA
KILIASMSIP  SIFEPMKIDG  EIYVDGLVSR  NLPVEEAYEM  GADIVVASDI
GAPVVEKDDY  NILSVMNQAS  TIQASNITKI  SREKASILIS  PDVKNISALD
SSKKEELMKL  GKVAAEKQID  KIKLLAKADN  KKKKEKFVTN  SDAKIIINKI
EYNDKFDKNT  VIVLNDIFKG  LLNNPISKKD  IDKKIIDVYS  SKYMDKVYYT
VDNGVLYLDG  EKAHHHHHH
```

D3

D1-3 (100%), 46 898,9 Da
Fusobacterium nucleatum (FplA) | Trunk T
28 exclusive unique peptides, 38 exclusive unique spectra, 208 total spectra, 231/419 amino acids (55% coverage)

```
MENIELKSRE  DVEIENLESQ  IKVLEDKIQT  IKKLKSAKDN  KNLKVALVLS
GGGVKGYAHL  GVLRVLEREN  IKIDYITGTS  IGAFIGTLYS  IGYTVDEIEK
FLDDVNVSNF  LETITDNTNL  SLEKKESLKK  YSVHLSFDNE  LNFSFPKGLR
GTGEAYLLLK  GLLGKYEHMD  NFDNFPIPLR  IIATNLNTGE  TKAFSKGDVA
KILIASMSIP  SIFEPMKIDG  EIYVDGLVSR  NLPVEEAYEM  GADIVVASDI
GAPVVEKDDY  NILSVMNQAS  TIQASNITKI  SREKASILIS  PDVKNISALD
SSKKEELMKL  GKVAAEKQID  KIKLLAKADN  KKKKEKFVTN  SDAKIIINKI
EYNDKFDKNT  VIVLNDIFKG  LLNNPISKKD  IDKKIIDVYS  SKYMDKVYYT
VDNGVLYLDG  EKAHHHHHH
```

E1

E1-3/F1 (100%), 35 042,6 Da
Ralstonia solanacearum PLA | Trunk T
14 exclusive unique peptides, 24 exclusive unique spectra, 81 total spectra, 179/329 amino acids (54% coverage)

```
MHGQSAASPP  SAQDDVRRPR  IGLVLSGGGA  RGYAHIGVLK  MLERLRVPID
AIAGTSMGAV  VGGLYASGLH  ADALEQRLSQ  VNLSDIAFDR  KERAKLPQSL
REDDFQYPIG  LSAGYANGAF  KLPAGLVQGN  RLLALLKIWT  AQWPDNIDFA
HLPIPFRAMA  TDLATGDGVV  LDHGSLALAM  RASMAVPGLF  APIEVDGRTL
VDGGLVSNLP  VQLARDMGVD  IVIAVNIGSD  LQRPDALASP  AAVTEQMITI
LVGQNVRAQK  ALLHRSDVLL  EPRLTDLSFT  DFAKGPQGVH  AGEEAVVDAQ
ARLAALSLSP  QAYAAYREAH  RPQHHHHHH
```

E2

E1-3/F1 (100%), 35 042,6 Da
Ralstonia solanacearum PLA | Trunk T
8 exclusive unique peptides, 11 exclusive unique spectra, 32 total spectra, 114/329 amino acids (35% coverage)

```
MHGQSAASPP  SAQDDVRRPR  IGLVLSGGGA  RGYAHIGVLK  MLERLRVPID
AIAGTSMGAV  VGGLYASGLH  ADALEQRLSQ  VNLSDIAFDR  KERAKLPQSL
REDDFQYPIG  LSAGYANGAF  KLPAGLVQGN  RLLALLKIWT  AQWPDNIDFA
HLPIPFRAMA  TDLATGDGVV  LDHGSLALAM  RASMAVPGLF  APIEVDGRTL
VDGGLVSNLP  VQLARDMGVD  IVIAVNIGSD  LQRPDALASP  AAVTEQMITI
LVGQNVRAQK  ALLHRSDVLL  EPRLTDLSFT  DFAKGPQGVH  AGEEAVVDAQ
ARLAALSLSP  QAYAAYREAH  RPQHHHHHH
```

E3

E1-3/F1 (100%), 35 042,6 Da
Ralstonia solanacearum PLA | Trunk T
12 exclusive unique peptides, 16 exclusive unique spectra, 43 total spectra, 150/329 amino acids (46% coverage)

```
MHGQSAASPP  SAQDDVRRPR  IGLVLSGGGA  RGYAHIGVLK  MLERLRVPID
AIAGTSMGAV  VGGLYASGLH  ADALEQRLSQ  VNLSDIAFDR  KERAKLPQSL
REDDFQYPIG  LSAGYANGAF  KLPAGLVQGN  RLLALLKIWT  AQWPDNIDFA
HLPIPFRAMA  TDLATGDGVV  LDHGSLALAM  RASMAVPGLF  APIEVDGRTL
VDGGLVSNLP  VQLARDMGVD  IVIAVNIGSD  LQRPDALASP  AAVTEQMITI
LVGQNVRAQK  ALLHRSDVLL  EPRLTDLSFT  DFAKGPQGVH  AGEEAVVDAQ
ARLAALSLSP  QAYAAYREAH  RPQHHHHHH
```

F1

E1-3/F1 (100%), 35 042,6 Da
Ralstonia solanacearum PLA | Trunk T
5 exclusive unique peptides, 5 exclusive unique spectra, 14 total spectra, 58/329 amino acids (18% coverage)

```
MHGQSAASPP  SAQDDVRRPR  IGLVLSGGGA  RGYAHIGVLK  MLERLRVPID
AIAGTSMGAV  VGGLYASGLH  ADALEQRLSQ  VNLSDIAFDR  KERAKLPQSL
REDDFQYPIG  LSAGYANGAF  KLPAGLVQGN  RLLALLKIWT  AQWPDNIDFA
HLPIPFRAMA  TDLATGDGVV  LDHGSLALAM  RASMAVPGLF  APIEVDGRTL
VDGGLVSNLP  VQLARDMGVD  IVIAVNIGSD  LQRPDALASP  AAVTEQMITI
LVGQNVRAQK  ALLHRSDVLL  EPRLTDLSFT  DFAKGPQGVH  AGEEAVVDAQ
ARLAALSLSP  QAYAAYREAH  RPQHHHHHH
```

G1

G1 (100%), 34 242,8 Da
Aeromonas hydrophila PLA | Trunk T
15 exclusive unique peptides, 22 exclusive unique spectra, 261 total spectra, 169/317 amino acids (53% coverage)

```
MAAQSERPKI  ALVLSGGGAK  GAAHIGILKV  LEEKRIPVDI  IVGTSMGSYV
AGMYAMGLSA  EEVERTTLAI  DWNKGYQDKV  GRDELSLRKK  QQSEQYQLRT
DIGVNGDSVQ  FPDGFFQGQS  MASLLRHATS  NLPVQKSFDD  LPIPYRAMAT
DMETVTPFVL  DHGSLAKAMQ  ASMSIPGALK  PVEWEGHILA  DGGTVNNMPV
DVAKAMGADV  VIAVDISAKL  RTRESLKSGL  AMIDQLTTYM  TQVGTEKQKA
LMGPRDVLLT  PEFGNMGIAD  FALMPEGIKL  GEQVANRASA  QLDALSLSPA
AYTAYRNQKL  SHHHHHH
```

G2

G1 (100%), 34 242,8 Da
Aeromonas hydrophila PLA | Trunk T
17 exclusive unique peptides, 32 exclusive unique spectra, 217 total spectra, 226/317 amino acids (71% coverage)

```
MAAQSERPKI  ALVLSGGGAK  GAAHIGILKV  LEEKRIPVDI  IVGTSMGSYV
AGMYAMGLSA  EEVERTTLAI  DWNKGYQDKV  GRDELSLRKK  QQSEQYQLRT
DIGVNGDSVQ  FPDGFFQGQS  MASLLRHATS  NLPVQKSFDD  LPIPYRAMAT
DMETVTPFVL  DHGSLAKAMQ  ASMSIPGALK  PVEWEGHILA  DGGTVNNMPV
DVAKAMGADV  VIAVDISAKL  RTRESLKSGL  AMIDQLTTYM  TQVGTEKQKA
LMGPRDVLLT  PEFGNMGIAD  FALMPEGIKL  GEQVANRASA  QLDALSLSPA
AYTAYRNQKL  SHHHHHH
```

Figure S5. A) SDS-PAGE of BS3 crosslinked PlAs. Highlighted in red are high molecular weigth bands (A1-G2) chosen for MS. B) MS data confirming PlA nature of high molecular weight bands, labelled A1-G2, observed in the PlA crosslinking experiment. Reference sequence indicated above the individual result. Peptides detected by MS shown in yellow.

Table S1. Direct toxic effect of AhPlA, BpPlA, FplA and PlpD. Shown is the percental survival of *Galleria mellonella*. LD_{50}(AhPlA)=509 µg/g; LD_{50}(BpPlA)=13,9 mg/g.

	Days past infection	**AhPlA**			**AhPlA S67A D213N**	**BpPlA**			**BpPlA S230A D378N**	**FplA**			**PlpD**	**PBS**
Conc./Bodyweight [µg/g]		**2**	**20**	**200**	**200**	**2**	**20**	**200**	**200**	**1,25**	**12,5**	**125**	**400**	**-**
n		**8**	**16**	**15**	**10**	**8**	**16**	**18**	**13**	**8**	**8**	**8**	**8**	**5**
	0	100	100	100	100	100	100	94	100	100	100	100	100	100
	1	100	88	87	100	100	88	89	92	100	100	100	100	100
	2	100	88	73	100	100	88	89	92	100	100	100	100	100
	3	100	81	73	100	100	81	89	92	100	100	100	100	100
	4	100	81	73	100	100	81	83	92	100	100	100	100	100
	5	100	75	60	100	100	81	78	92	100	100	100	100	100